J|A|C|S
ARTICLES
Published on Web 07/09/2002

# Crystal Engineering for Topochemical Polymerization of Muconic Esters Using Halogen−Halogen and CH/$\pi$ Interactions as Weak Intermolecular Interactions

Akikazu Matsumoto,*[,†,‡] Toshihiro Tanaka,[‡] Takashi Tsubouchi,[†] Kohji Tashiro,[§] Seishi Saragai,[§] and Shinsuke Nakamoto[§]

*Contribution from the Department of Applied Chemistry, Graduate School of Engineering, Osaka City University, PRESTO, Japan Science and Technology Corporation (JST), Conversion and Control by Advanced Chemistry, Sugimoto, Sumiyoshi-ku, Osaka 558-8585, Japan, and the Department of Macromolecular Science, Graduate School of Science, Osaka University, Toyonaka, Osaka 560-0043, Japan*

Received April 12, 2002

***Abstract:*** We now report the molecular and crystal structure design of muconic ester derivatives on the basis of crystal engineering using halogen−halogen contacts and CH/$\pi$ interactions. The solid-state photoreaction pathway of the dibenzyl (*Z*,*Z*)-muconates as the 1,3-diene dicarboxylic acid monomers depends on the structure of the ester groups. The substitution of a halogen atom for the aromatic hydrogen of a benzyl group induces topochemical polymerization to produce stereoregular polymers in a crystalline form, whereas the unsubstituted benzyl derivative isomerizes to yield the corresponding *E*,*E* isomer under similar conditions. The topochemical polymerization process is directly confirmed by the fact that the single-crystal structures before and after the polymerization are very similar to each other. From the crystal structure analysis for a series of substituted benzyl (*Z*,*Z*)- and (*E*,*E*)-muconates, it has been revealed that the planar diene moieties are closely packed to form a columnar structure in the crystals. The stacking of the polymerizable monomers is characterized by a stacking distance of 4.9−5.2 Å along the columns. This structure is supported by a halogen−halogen interaction between the chlorine or bromine atoms introduced at the p position of the benzyl groups in addition to an aromatic stacking due to the CH/$\pi$ interaction between the benzylic methylene hydrogens and aromatic rings. The design of a monomer packing corresponds to the type and position of the introduced halogen atom and also the polymorphs. To make a stacking distance of 5 Å using both halogen−halogen and CH/$\pi$ interactions as supramolecular synthons is important for the molecular design of muconic ester derivatives appropriate for topochemical polymerization.

## Introduction

Crystal engineering is the planning and construction of the structure and properties of crystalline materials by designing molecular building blocks.[1−5] Topochemical polymerization is one of the most powerful and promising methods for controlling the structures of both the polymer chains and crystals,[6,7] because all the included reactions are highly regulated under a crystal lattice control, and consequently, polymers are obtained in a crystalline form as reaction products. A topochemical polymerization process requires the favorable prearrangement of monomer molecules in the crystals, but molecules are arranged as a result of accumulated intermolecular interactions and packed so close as to leave a minimal volume of empty space in the crystals. Therefore, the ab initio and precise prediction of crystal structures from molecular formulas is still difficult, and the fabrication of a designer crystal structure has been a challenging topic.[8,9] In the past decade, however, directional and strong intermolecular interactions, such as hydrogen bonds, X−H···X (X = O, N), has overcome such problems of controlling an interaction between mutual molecules and taming a capricious crystal structure. Strong hydrogen bonds are most commonly

* Corresponding author. Fax: +81-6-6605-2981. E-mail: matsumoto@a-chem.eng.osaka-cu.ac.jp.
† Dept. of Applied Chemistry.
‡ PRESTO-JST.
§ Dept. of Macromolecular Science.

(1) Desiraju, G. R. *Crystal Engineering: The Design of Organic Solids*; Elsevier: Amsterdam, 1989.
(2) *Comprehensive Supramolecular Chemistry*, *Vol. 6, Solid State Supramolecular Chemistry: Crystal Engineering*; MacNicol, D. D., Toda, F., Bishop, R., Eds.; Pergamon: Oxford, 1996.
(3) Steed, J. W.; Atwood, J. L. *Supramolecular Chemistry*; Wiley: Chichester, 2000; pp 389−462.
(4) *The Crystal as a Supramolecular Entity: Perspective in Supramolecular Chemistry Vol. 2*; Desiraju, G. R., Ed.; Wiley: Chichester, 1995.
(5) *Topics in Current Chemistry, Vol. 198, Design of Organic Solids*; Weber, E., Vol. Ed.; Springer: Berlin, 1998.
(6) (a) Schmidt, G. M. J. *Pure Appl. Chem.* **1971**, *27*, 647−678. (b) Wegner, G. *Pure Appl. Chem.* **1977**, *49*, 443−454. (c) Bässler, H. *Adv. Polym. Sci.* **1984**, *63*, 1−48. (d) Enkelmann, V. *Adv. Polym. Sci.* **1984**, *63*, 91−136. (e) Tieke, B. *Adv. Polym. Sci.* **1985**, *71*, 79−151. (f) Hasegawa, M. *Adv. Phys. Org. Chem.* **1995**, *30*, 117−171.
(7) Matsumoto, A.; Odani, T. *Macromol. Rapid Commun.* **2001**, *22*, 1195−1215.
(8) (a) Kitaigorodskii, A. I. *Molecular Crystals and Molecules*; Academic Press: New York, 1973. (b) Kitaigorodskii, A. I. *Mixed Crystals*; Solid-State Science Vol. 33; Springer: Berlin, 1984.
(9) (a) Gavezzotti, A. *Acc. Chem. Res.* **1994**, *27*, 309−314. (b) *Crystal Engineering: From Molecules and Crystals to Materials*; Braga, D., Grepioni, F., Orpen, A. G., Eds.; NATO Science Series C, Vol. 538; Kluwer: Dordrecht, 1999.

used for the controlled molecular packing to realize a rational design for the crystal structure of organic solids in the context of crystal engineering and supramolecular chemistry.[1−5,10]

When diethyl (*Z*,*Z*)-muconate (EMU) [diethyl (*Z*,*Z*)-2,4-hexadienedioate] is irradiated with UV light, sunlight, X-, and $\gamma$-rays in the crystalline state, polymerization proceeds via a radical mechanism to give highly stereoregular polymers consisting of *meso*-diisotactic-*trans*-2,5-repeating units.[7,11] We have already revealed the features and mechanism of the topochemical polymerization of EMU in the crystalline state using IR, Raman, NMR, and ESR spectroscopies, as well as X-ray diffraction experiments.[11−13] The single-crystal structure of the EMU monomer was determined by X-ray structure analysis with a charge-coupled device (CCD) camera system as a two-dimensional detector and evidenced the topochemical process of the EMU polymerization.[12b] In contrast, no other polymerizable esters other than EMU have been found. Some esters have no reaction, whereas others induce photoisomerization to yield the corresponding *E*,*E* isomers, but do not produce any stereoregular polymer. Recently, we also revealed that EMU does not polymerize at all below −45 °C because of a structural change accompanying the first-order phase transition.[14] The crystal structures of EMU at both room temperature and −80 °C are similar to each other; i.e., they have the same space group and similar cell parameters. The molecular geometry and packing in the crystal at a low temperature are essentially the same as that of the high-temperature phase, except for the fact that the *b* axial length is contracted by about 14% at the low temperature in the direction of the polymer chain formation. This suggests that the topochemical polymerization of the muconates is sensitive to a slight change in the molecular packing, and therefore, such a structural limit is a hurdle for the design and control of the topochemical polymerization of the other alkyl esters.

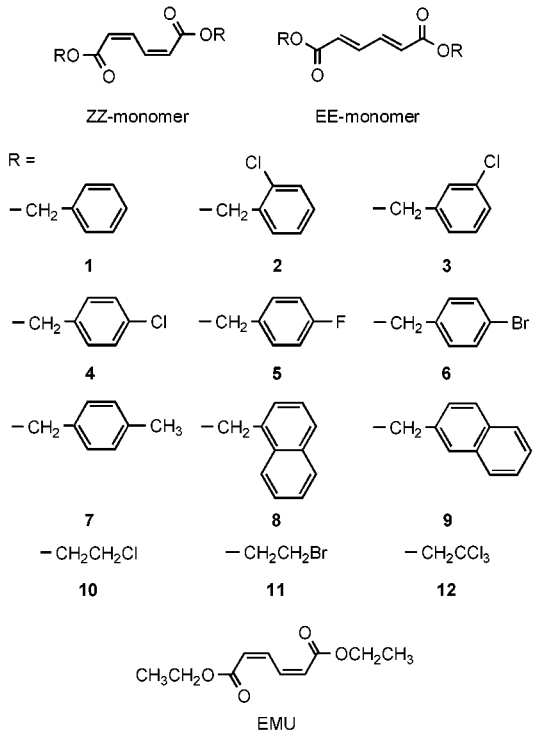


***Figure 1.*** Chemical structures of monomers used in this study.

Differing from the difficulty of the ester derivative polymerizations, several alkyl- ammonium (*Z*,*Z*)-muconates, such as the *n*-alkyl-, benzyl-, and 1-naphthylmethylammonium salts photopolymerize under UV irradiation in the crystalline state.[15] An X-ray crystal structure analysis has revealed a relationship between the molecular packing in the crystals and topochemical polymerization reactivity. The crystal structures of the benzylammonium muconates are classified into columnar and sheet types on the basis of the molecular arrangement in the crystals.[15a] Both types involve two-dimensional hydrogen bond networks between the primary ammonium cations and carboxylate anions. In the former structure, the stacking of the diene moieties is suitable for topochemical polymerization, whereas the latter has a molecular packing favoring isomerization or no reaction. More recently, sophisticated molecular design based on polymer crystal engineering realized the topochemical polymerization of not only (*Z*,*Z*)- but also the (*E*,*E*)-1,3-diene mono- or dicarboxylic acid derivatives bearing a naphthylmethylammonium group as the countercation.[16] In the crystals of the naphthylmethylammonium derivatives, the two-dimensional hydrogen bond network and the herringbone stacking of the naphthyl moieties are important for producing a robust and desired crystal structure.

How can we design the crystal structure for the ester derivatives possessing no hydrogen bond network? Desiraju et al. coined the concept of supramolecular synthons, which are attractive intermolecular interactions useful for a rational crystal design.[17,18] Not only strong interactions, such as a hydrogen bond, but also $\pi-\pi$ stacking,[18a] weak hydrogen bonds,[19] such

(10) (a) Ermer, O. *J. Am. Chem. Soc*. **1988**, *110*, 3747−3754. (b) Simard, M.; Su, D.; Wuest, J. D. *J. Am. Chem. Soc*. **1991**, *113*, 4696−4698. (c) Aakeröy, C. B.; Seddon, K. R. *Chem. Soc. Rev*. **1993**, *22*, 397−407. (d) Zaworotko, M. J. *Chem. Soc. Rev*. **1994**, *23*, 283−288. (e) Russell, V. A.; Etter, M. C.; Ward, M. D. *J. Am. Chem. Soc*. **1994**, *116*, 1941−1952. (f) Endo, K.; Sawaki, T.; Koyanagi, M.; Kobayashi, K.; Masuda, H.; Aoyama, Y. *J. Am. Chem. Soc*. **1995**, *117*, 8341−8352. (g) Ung, A. T.; Gizachew, D.; Bishop, R.; Scudder, M. L.; Dance, I. G.; Craig, D. C. *J. Am. Chem. Soc*. **1995**, *117*, 8745−8756. (h) Miyata, M.; Sada, K. *Comprehensive Supramolecular Chemistry*, *Vol. 6*, *Solid State Supramolecular Chemistry: Crystal Engineering*; MacNicol, D. D., Toda, F., Bishop, R., Eds.; Pergamon: Oxford, 1996; pp 147−176. (i) Russell, V. A.; Ward, M. D. *Chem. Mater*. **1996**, *8*, 1654−1666. (j) Kinbara, K.; Hashimoto, Y.; Sukegawa, M.; Nohira, H.; Saigo, K. *J. Am. Chem. Soc*. **1996**, *118*, 3441−3449. (k) Melendez, R. E.; Sharma, C. V. K.; Zaworotko, M. J.; Bauer, C.; Rogers, R. D. *Angew. Chem., Int. Ed. Engl*. **1996**, *35*, 2213−2215. (l) Aakeröy, C. B. *Acta Crystallogr*. **1997**, *B53*, 569−586. (m) Braga, D.; Grepioni, F. *Acc. Chem. Res*. **1997**, *30*, 81−87. (n) Russell, V. A.; Evans, C. C., Li, W.; Ward, M. D. *Science* **1997**, *276*, 575−579. (o) Brunet, P.; Simard, M.; Wuest, J. D. *J. Am. Chem. Soc*. **1997**, *119*, 2737−2738. (p) Braga, D.; Grepioni, F.; Desiraju, G. R. *Chem. Rev*. **1998**, *98*, 1375−1405. (q) Holman, K. T.; Pivovar, A. M.; Swift, J. A.; Ward, M. D. *Acc. Chem. Res*. **2001**, *34*, 107−118. (r) Holman, K. T.; Pivovar, A. M.; Ward, M. D. *Science* **2001**, *294*, 1907−1911. (s) Moulton, B.; Zaworotko, M. J. *Chem. Rev*. **2001**, *101*, 1629−1658. (t) Beatty, A. M. *Cryst. Eng. Comm*. **2001**, *51*, 1−13. (u) Sada, K.; Sugahara, M.; Kato, K.; Miyata, M. *J. Am. Chem. Soc*. **2001**, *123*, 4386−4392.

(11) (a) Matsumoto, A.; Matsumura, T.; Aoki, S. *J. Chem. Soc., Chem. Commun*. **1994**, 1389−1390. (b) Matsumoto, A.; Yokoi, K.; Aoki, S.; Matsumoto, A.; Tashiro, K.; Kamae, T.; Kobayashi, M. *Macromolecules* **1998**, *31*, 2129−2136. (c) Matsumoto, A.; Katayama, K.; Odani, T.; Oka, K.; Tashiro, K.; Saragai, S.; Nakamoto, S. *Macromolecules* **2000**, *33*, 7786−7792.

(12) (a) Tashiro, K.; Kamae, T.; Kobayashi, M.; Matsumoto, A.; Yokoi, K.; Aoki, S. *Macromolecules* **1999**, *32*, 2449−2454. (b) Tashiro, K.; Zadorin, A. N.; Saragai, S.; Kamae, T.; Matsumoto, A.; Yokoi, K.; Aoki, S. *Macromolecules* **1999**, *32*, 7946−7950.

(13) Saragai, S.; Tashiro, K.; Nakamoto, S.; Matsumoto, A.; Tsubouchi, T. *J. Phys. Chem. B* **2001**, *105*, 4155−4165.

(14) Saragai, S.; Tashiro, K.; Nakamoto, S.; Kamae, T.; Matsumoto, A.; Tsubouchi, T. *Polym. J*. **2001**, *33*, 199−203.

(15) (a) Matsumoto, A.; Odani, T.; Chikada, M.; Sada, K.; Miyata, M. *J. Am. Chem. Soc*. **1999**, *121*, 11122−11129. (b) Matsumoto, A.; Odani, T.; Sada, K.; Miyata, M.; Tashiro, K. *Nature* **2000**, *405*, 328−330. (c) Odani, T.; Matsumoto, A. *Macromol. Rapid Commun*. **2000**, *21*, 40−44. (d) Nagahama, S.; Matsumoto, A. *J. Am. Chem. Soc*. **2001**, *123*, 12176−12181.

(16) Matsumoto, A.; Nagahama, S.; Odani, T. *J. Am. Chem. Soc*. **2000**, *122*, 9109−9119.

***Table 1.*** Photoreaction of Muconic Esters in the Crystalline State[a]

| run | monomer | ester alkyl group | crystal habit | mp (°C) | photoproduct | yield (%) |
|---|---|---|---|---|---|---|
| 1 | (*Z*,*Z*)-**1** | benzyl | needles | 67.2−67.6 | *E*,*E* isomer | 31 |
| 2 | (*Z*,*Z*)-**2**-I | 2-chlorobenzyl | needles | 75.1−75.7 | polymer | *b* |
| 3 | (*Z*,*Z*)-**2**-II | 2-chlorobenzyl | needles | 75.7−76.1 | no reaction | |
| 4 | (*Z*,*Z*)-**3** | 3-chlorobenzyl | needles | 100.8−101.1 | no reaction | |
| 5 | (*Z*,*Z*)-**4** | 4-chlorobenzyl | plates | 130.8−131.0 | polymer | 97 |
| 6 | (*Z*,*Z*)-**5** | 4-fluorobenzyl | plates | 113.6−113.9 | no reaction | |
| 7 | (*Z*,*Z*)-**6**-I | 4-bromobenzyl | plates | 142.0−142.4 | polymer | 87 |
| 8 | (*Z*,*Z*)-**6**-II | 4-bromobenzyl | prisms | 142.2−143.1 | no reaction | |
| 9 | (*Z*,*Z*)-**7** | 4-methylbenzyl | prisms | 103.5−103.6 | no reaction | |
| 10 | (*Z*,*Z*)-**8** | 1-naphthylmethyl | plates | 122.0−122.2 | *E*,*E* isomer | 41 |
| 11 | (*Z*,*Z*)-**9** | 2-naphthylmethyl | powder | 157.7−158.1 | *E*,*E* isomer | 58 |
| 12 | (*Z*,*Z*)-**10** | 2-chloroethyl | plates | 104.1−105.0 | *E*,*E* isomer | 19 |
| 13 | (*Z*,*Z*)-**11** | 2-bromoethyl | plates | 97.1−98.2 | *E*,*E* isomer | 10 |
| 14 | (*Z*,*Z*)-**12** | 2,2,2-trichloroethyl | plates | 124.3−125.2 | *E*,*E* isomer | 1 |
| 15 | (*E*,*E*)-**1** | benzyl | needles | 106.4−106.9 | no reaction | |
| 16 | (*E*,*E*)-**2** | 2-chlorobenzyl | prisms | 99.4−102.3 | no reaction | |
| 17 | (*E*,*E*)-**3** | 3-chlorobenzyl | prisms | 101.9−102.6 | no reaction | |
| 18 | (*E*,*E*)-**4** | 4-chlorobenzyl | powder | 153.6−156.8 | no reaction | |
| 19 | (*E*,*E*)-**5** | 4-fluorobenzyl | powder | 113.4−114.1 | no reaction | |
| 20 | (*E*,*E*)-**6** | 4-bromobenzyl | prisms | 143.1−147.4 | no reaction | |
| 21 | (*E*,*E*)-**7** | 4-methylbenzyl | needles | 132.1−135.7 | no reaction | |
| 22 | (*E*,*E*)-**8** | 1-naphthylmethyl | powder | 164.3−164.9 | no reaction | |
| 23 | (*E*,*E*)-**9** | 2-naphthylmethyl | plates | 181.8−182.4 | no reaction | |

[a] Monomers were recrystallized from chloroform. UV irradiation was carried out with a high-pressure Hg lamp (100 W) at a distance of 10 cm at room temperature for 8 h. Polymers were isolated as insoluble products. Isomerization yield was determined by $^1$H NMR spectroscopy. [b] Not determined as a result of contamination with (*Z*,*Z*)-**2**-II.

as C−H···X (X = O, N)[19,20] or X−H···$\pi$ (X = C, O, N),[21,22]and halogen[23−25] or sulfur[19] atom interactions are used for the orientation of molecules in a crystal. These strong and weak intermolecular interactions have been exploited as the non-covalent interactions in the context of crystal engineering. In the crystals of the ester derivatives of muconic acid, the crystal structure and the stacking of monomers are possibly controlled by weak interactions instead of strong hydrogen bonding. To systematically investigate the crystal structure and the molecular packing of a series of derivatives bearing selected substituents is important for the rational design of a crystal structure and its reactivity. Recently, we found that the introduction of halogen atoms into the benzyl moiety of muconic esters induces a topochemical polymerization and that weak interaction involving halogen−halogen contact as well as CH/$\pi$ interactions are important for constructing the crystal structure of the monomers. In this paper, we discuss the weak intermolecular interactions between muconate molecules having aromatic moieties, halogen atoms, or both in the ester groups, as shown in Figure 1, for the crystal engineering of muconic ester polymerization.

## Results

**Photoreaction.** The monomer crystals were obtained as needles, plates, prisms, or powder after recrystallization from chloroform. The crystals of (*Z*,*Z*)-**2** and (*Z*,*Z*)-**6** were isolated as polymorphs. (*Z*,*Z*)-**2**-I was crystallized as thin needles during rapid evaporation of the solvent on a glass plate. It tended to be contaminated with another polymorph, (*Z*,*Z*)-**2**-II, which was quantitatively obtained by slow evaporation. Each crystal of (*Z*,*Z*)-**6** with a different appearance ((*Z*,*Z*)-**6**-I as the plates and (*Z*,*Z*)-**6**-II as the prisms) was preferentially prepared by recrystallization at room temperature by seeding. The photoirradiation was carried out using a high-pressure mercury lamp at room temperature for 8 h. The photoreactivity of these monomers in the crystalline state is summarized in Table 1.

A few selected crystals of the *Z*,*Z* monomers gave an insoluble photoproduct in 87−97% yield during UV irradiation (runs 5 and 7 in Table 1). IR spectroscopy supports the formation of a polymer with a trans-2,5 structure as the repeating unit. A peak due to the conjugating diene at 1588 cm$^{-1}$

(17) (a) Etter, M. C. *Acc. Chem. Res*. **1990**, *23*, 120−126. (b) Etter, M. C. *J. Phys. Chem.* **1991**, *95*, 4601−4610. (c) Etter, M. C.; MacDonald, J. C.; Bernstein, J. *Acta Crystallogr.* **1990**, *B46*, 256−262.
(18) (a) Desiraju, G. R.; Gavezzotti, A. *J. Chem. Soc., Chem. Commun.* **1989**, 621−623. (b) Desiraju, G. R. *Acc. Chem. Res.* **1991**, *24*, 290−296. (c) Desiraju, G. R. *Angew. Chem., Int. Ed. Engl.* **1995**, *34*, 2311−2327. (d) Desiraju, G. R. *Nature* **2001**, *412*, 397−400.
(19) Desiraju, G. R.; Steiner, T. *The Weak Hydrogen Bond in Structural Chemistry and Biology*; Oxford University Press: Oxford, 1999.
(20) Desiraju, G. R. *Acc. Chem. Res.* **1996**, *29*, 441−449.
(21) (a) Nishio, M.; Hirota, M.; Umezawa, Y. *The CH/π Interaction: Evidence, Nature, and Consequences*; Wiley: New York, 1998. (b) Nishio, M.; Umezawa, Y.; Hirota, M.; Takeuchi, Y. *Tetrahedron* **1995**, *51*, 8665−8701. (c) Umezawa, Y.; Tsuboyama, S.; Honda, K.; Uzawa, J.; Nishio, M. *Bull. Chem. Soc. Jpn*. **1997**, *71*, 1207−1213. (d) For comprehensive literature list for the CH/$\pi$ interaction, see http://www.tim.hi-ho.ne.jp/dionisio/.
(22) (a) Kobayashi, K.; Asakawa, Y.; Kato, Y.; Aoyama, Y. *J. Am. Chem. Soc*. **1992**, *114*, 10307−10313. (b) Kobayashi, K.; Asakawa, Y.; Kikuchi, Y.; Toi, H.; Aoyama, Y. *J. Am. Chem. Soc.* **1993**, *115*, 2648−2654. (c) Hunter, R.; Haueosen, R. H.; Irving, A. *Angew. Chem., Int. Ed. Engl*. **1994**, *33*, 566−568. (d) Muller, T. E.; Mingos, D. M. P.; Williams, D. J. *J. Chem. Soc., Chem. Commun*. **1994**, 1787−1788. (e) Bohmer, V. *Angew. Chem., Int. Ed. Engl*. **1995**, *34*, 713−745. (f) Timmerman, P.; Verboom, W.; Reinhoudt, D. N. *Tetrahedron* **1996**, *52*, 2663−2704. (g) Grillard, R. E.; Raymo, F. M.; Stoddart, J. F. *Chem. Eur. J.* **1997**, *3*, 1933−1940. (h) Weiss, H. C.; Blaser, D.; Boese, R.; Doughan, B. M.; Haley, M. M. *Chem. Commun.* **1997**, 1703−1704. (i) Tsuzuki, S.; Honda, K.; Uchimaru, T.; Mikami, M.; Yanabe, K. *J. Am. Chem. Soc*. **2000**, *122*, 3746−3753.
(23) (a) Taylor, R.; Kennard, O. *J. Am. Chem. Soc*. **1982**, *104*, 5063−5070. (b) Rowland, R. S.; Taylor, R. *J. Phys. Chem.* **1996**, *100*, 7384−7391.
(24) (a) Williams, D. E.; Hsu, L.-Y. *Acta Crystallogr*. **1985**, *A41*, 296−301. (b) Ranasubbu, N.; Parthasarathy, R.; Murray-Rust, P. *J. Am. Chem. Soc*. **1986**, *108*, 4308−4314. (c) Price, S. L.; Stone, A. J.; Lucas, J.; Rowland, R. S.; Thornley, A. E. *J. Am. Chem. Soc*. **1994**, *116*, 4910−4918. (d) Lommerse, J. P. M.; Stone, A. J.; Taylor, R.; Allen, F. H. *J. Am. Chem. Soc*. **1996**, *118*, 3108−3116. (e) Navon, O.; Bernstein, J.; Khodorkovsky, V. *Angew. Chem., Int. Ed. Engl*. **1997**, *36*, 601−603. (f) Venkatesan, K.; Ramamurthy, V. *Photochemistry in Organized and Constrained Media*; Ramamurthy, V., Ed.; VCH: Berlin, 1991; pp 1133−1184. (g) Thalladi, V. R.; Weiss, H.-C.; Boese, R.; Nangia, A.; Desiraju, G. R. *Acta Crystallogr*. **1999**, *B55*, 1005−1013.
(25) Goldberg, I.; Krupitsky, H.; Stein, Z.; Hsiou, Y.; Strouse, C. E. *Supramol. Chem*. **1994**, *4*, 203−221. (b) Broder, C. K.; Howard, J. A.; Keen, D. A.; Wilson, C. C.; Allen, F. H.; Jetti, R. K.; Nangia, A.; Desiraju, G. R. *Acta Crystallogr*. **2000**, *B56*, 1080−1084. (c) Tanaka, K.; Fujimoto, D.; Altreuther, A.; Oeser, T.; Irngartinger, H.; Toda, F. *J. Chem. Soc., Perkin Trans. 2* **2000**, 2115−2120.

***Scheme 1***

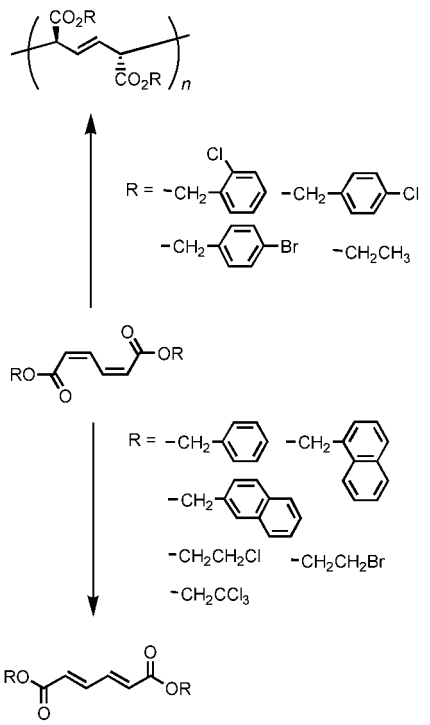


disappeared and the out-of-plane deformation vibration due to the *trans*-CH═CH moiety was observed at 982 $cm^{-1}$ after UV irradiation. A change in the IR spectrum is identical to the previously reported results for the polymerization of the related derivatives.[11,12] All of the polymers obtained from the benzyl esters were insoluble in all solvents, whereas poly(EMU) is soluble in trifluoroacetic acid and 1,1,1,3,3,3-hexafluoro-2-propanol. All attempts to hydrolyze the benzyl ester polymers and also to transform them into other esters failed.

The unsubstituted benzyl (run 1) and 1- and 2-naphthylmethyl esters (runs 10 and 11) of the *Z*,*Z* derivatives isomerized to the corresponding *E*,*E* isomer in 31−58% conversion. The halogen-substituted ethyl esters also provided the *E*,*E* isomers (runs 12−14). The other *Z*,*Z* derivatives as well as all the *E*,*E* derivatives were inert during the photoirradiation. Scheme 1 summarizes the photoreaction pathway of the (*Z*,*Z*)-muconates in the crystalline state on the basis of the structure of the ester groups.

Figure 2 shows the result of the time-resolved measurement of the IR spectrum during the photoirradiation of (*Z*,*Z*)-**4**. The IR spectrum consists of two chemical components of the monomer and polymer, and both bands are distinguished. Therefore, the rate constant for the polymerization is simply determined from the increasing and decreasing intensities of the peaks. The intensity of the monomer band at 1588 $cm^{-1}$ decreases with an increasing UV irradiation time, and the intensities of the polymer bands at 982 and 718 $cm^{-1}$ increase. The polymerization approximately obeys the equation of the first-order reaction with regard to the monomer concentration (eq 1).[12a]

$$\ln C_1 = -kt \qquad (1)$$

Here, $C_1$ is the monomer fraction in the crystals, $k$ is the rate constant, and $t$ is the UV irradiation time. Figure 3 shows the relationship between ln $C_1$ and the photopolymerization time of (*Z*,*Z*)-**4**, (*Z*,*Z*)-**6**-I, and EMU in the crystalline state. The $k$

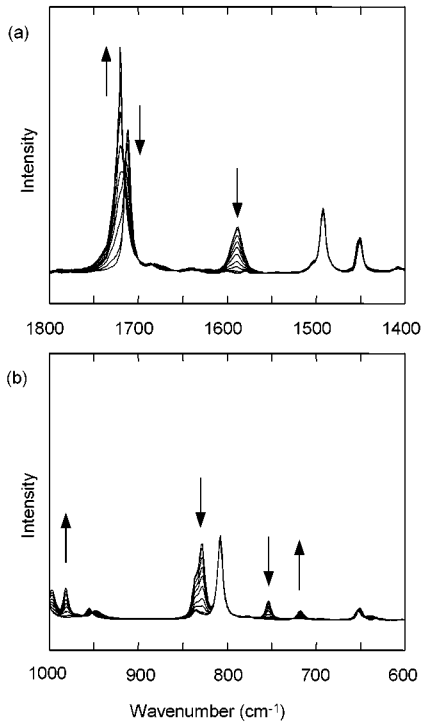


***Figure 2.*** Change in IR spectrum during the crystalline-state polymerization of (*Z*,*Z*)-**4** under UV irradiation with a high-pressure Hg lamp at room temperature. Irradiation time: 0, 1, 3, 5, 7, 10, 15, 20, 30, 45, and 60 min.

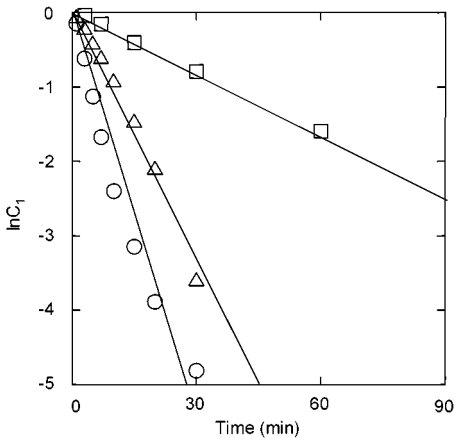


***Figure 3.*** Semilogarithmic plots of monomer fraction $C_1$ versus UV irradiation time during the photopolymerization in the crystalline state: (○) EMU, (△) (*Z*,*Z*)-**4**, and (□) (*Z*,*Z*)-**6**-I.

***Table 2.*** Rate Constants for Polymerization of (*Z*,*Z*)-Muconates in the Crystalline State[a]

| monomer | ester alkyl group | $k \times 10^3$ ($s^{-1}$) |
|---|---|---|
| EMU | ethyl | 3.39 ± 0.56 |
| (*Z*,*Z*)-**4** | 4-chlorobenzyl | 1.46 ± 0.34 |
| (*Z*,*Z*)-**6**-I | 4-bromobenzyl | 0.37 ± 0.14 |

[a] Irradiated with a high-pressure Hg lamp (100 W) at a distance of 20 cm at room temperature.

values determined from the slope of the lines are summarized in Table 2. The values decreased in the order of EMU > (*Z*,*Z*)-**4** > (*Z*,*Z*)-**6**-I.

**Single-Crystal Structure.** The crystallographic data for the X-ray single-crystal structure analysis are summarized in Table 3. The reflection from the crystals of the polymerizable monomers, (*Z*,*Z*)-**4** and (*Z*,*Z*)-**6**-I, was successfully collected

***Table 3.*** Crystallographic Data of Muconic Esters

| | Compd | | | | | | | |
|---|---|---|---|---|---|---|---|---|
| | (*Z*,*Z*)-**1**-II | (*Z*,*Z*)-**3** | (*Z*,*Z*)-**4** | | poly((*Z*,*Z*)-**4**) | (*Z*,*Z*)-**5** | (*Z*,*Z*)-**6**-I | (*Z*,*Z*)-**6**-II |
| formula | $C_{20}H_{18}O_4$ | $C_{20}H_{16}O_4Cl_2$ | $C_{20}H_{16}O_4Cl_2$ | | $C_{20}H_{16}O_4Cl_2$ | $C_{20}H_{16}O_4F_2$ | $C_{20}H_{16}O_4Br_2$ | $C_{20}H_{16}O_4Br_2$ |
| fw | 322.38 | 391.25 | 391.25 | | 391.25 | 358.34 | 480.15 | 480.15 |
| color | colorless | colorless | colorless | | colorless | colorless | colorless | colorless |
| crystal habit | needles | plates | plates | | plates | prisms | plates | prisms |
| crystal system | monoclinic | triclinic | monoclinic | | monoclinic | monoclinic | monoclinic | monoclinic |
| space group | $P2_1/c$ | $P\bar{1}$ | $P2_1/c$ | | $P2_1/c$ | $P2_1/c$ | $P2_1/c$ | $P2_1/n$ |
| *a*, Å | 8.571(5) | 8.458(2) | 5.629(6) | 5.6457(2) | 5.6796(3) | 11.459(5) | 5.68(1) | 8.049(1) |
| *b*, Å | 10.465(5) | 13.544(3) | 5.122(6) | 5.0639(3) | 4.8631(1) | 4.112(6) | 5.21(1) | 5.6585(6) |
| *c*, Å | 9.368(4) | 4.0436(5) | 32.08(2) | 31.685(4) | 32.097(1) | 18.705(5) | 32.26(7) | 21.477(3) |
| α, deg | | 93.971(7) | | | | | | |
| *β*, deg | 97.08(2) | 101.29(1) | 93.712(1) | 92.746(4) | 90.185(2) | 96.45(3) | 92.950(1) | 96.970(3) |
| *γ*, deg | | 78.737(8) | | | | | | |
| *V*, Å$^3$ | 838.9(7) | 445.2(1) | 923.0(4) | 904.82(8) | 886.54(5) | 875.8(1) | 953.0(4) | 970.9(2) |
| *Z* | 2 | 1 | 2 | 2 | 2 | 2 | 2 | 2 |
| $\rho_{calc}$, g/cm$^3$ | 1.284 | 1.459 | 1.408 | 1.436 | 1.466 | 1.359 | 1.673 | 1.642 |
| $\mu$(Mo Kα), cm$^{-1}$ | 0.89 | 3.87 | 3.74 | 3.81 | 3.89 | 1.08 | 42.74 | 42.08 |
| $2\theta_{max}$, deg | 33.88 | 54.9 | 20.36 | 55.0 | 54.9 | 55.0 | 15.84 | 55.0 |
| diffractometer | DIP3000 | RAXIS | Kappa-CCD | RAXIS | RAXIS | AFC7R | Kappa-CCD | RAXIS |
| reflections measured | 3681 | 2748 | 1373 | 5720 | 5572 | 2404 | 1360 | 3302 |
| unique reflections | 3553 | 1912 | 1370 | 2262 | 2098 | 2100 | 1360 | 1953 |
| $R_{merge}$ | | 0.021 | 0.000 | 0.047 | 0.034 | 0.301 | 0.000 | 0.023 |
| no. observed | 2507 | 1336 | 425 | 1806 | 1838 | 1099 | 129 | 1280 |
| | $I > 3\sigma(I)$ | $I > 2\sigma(I)$ | $I > \sigma(I)$ | $I > 2\sigma(I)$ | $I > 2\sigma(I)$ | $I > 2\sigma(I)$ | $I > 3\sigma(I)$ | $I > 2\sigma(I)$ |
| no. variables | 145 | 150 | 118 | 145 | 142 | 150 | 53 | 144 |
| parameter ratio | 17.29 | 8.91 | 3.60 | 12.46 | 12.94 | 7.33 | 2.44 | 8.89 |
| *R* | 0.063 | 0.052 | 0.081 | 0.070 | 0.066 | 0.050 | 0.083 | 0.049 |
| $R_w$ | 0.111 | 0.091 | 0.080 | 0.162 | 0.170 | 0.078 | 0.094 | 0.091 |
| GOF | 2.72 | 1.14 | 1.76 | 1.58 | 1.70 | 1.01 | 4.04 | 1.13 |
| temp, °C | 25 | 23 | 25 | −120 | 23 | 23 | 25 | 23 |
| final diff four map (e Å$^{-3}$) | 0.39, −0.58 | 0.19, −0.24 | 0.36, −0.33 | 0.39, −0.79 | 0.40, −0. 61 | 0.17, −0.29 | 0.54, −0.91 | 0.31, −0.34 |

| | Compd | | | | | | | |
|---|---|---|---|---|---|---|---|---|
| | (*Z*,*Z*)-**7** | (*Z*,*Z*)-**10** | (*Z*,*Z*)-**11** | (*E*,*E*)-**1**-I | (*E*,*E*)-**1**-II | (*E*,*E*)-**2** | (*E*,*E*)-**3** | (*E*,*E*)-**6** |
| formula | $C_{22}H_{22}O_4$ | $C_{10}H_{12}O_4Cl_2$ | $C_{10}H_{12}O_4Br_2$ | $C_{20}H_{18}O_4$ | $C_{20}H_{18}O_4$ | $C_{20}H_{16}O_4Cl_2$ | $C_{20}H_{16}O_4Cl_2$ | $C_{20}H_{16}O_4Br_2$ |
| fw | 350.41 | 267.11 | 356.01 | 322.38 | 322.38 | 391.25 | 391.25 | 480.15 |
| color | colorless | colorless | colorless | colorless | colorless | colorless | colorless | colorless |
| crystal habit | prisms | plates | plates | plates | needles | prisms | prisms | prisms |
| crystal system | triclinic | monoclinic | monoclinic | monoclinic | orthorhombic | monoclinic | monoclinic | monoclinic |
| space group | $P\bar{1}$ | $P2_1/a$ | $P2_1/a$ | $P2_1/c$ | $P2_12_12_1$ | $P2_1/n$ | $P2_1/a$ | $C2/c$ |
| *a*, Å | 5.4658(5) | 8.0986(1) | 8.3045(9) | 9.15(2) | 5.766(2) | 6.015(4) | 9.373(2) | 23.593(3) |
| *b*, Å | 7.6205(4) | 5.4164(3) | 5.5002(7) | 5.706(6) | 8.86(1) | 8.415(5) | 10.665(2) | 5.6741(8) |
| *c*, Å | 11.7151(7) | 13.8414(5) | 13.840(2) | 16.96(2) | 32.98(2) | 18.080(5) | 9.906(2) | 16.123(2) |
| α, deg | 103.828(6) | | | | | | | |
| *β*, deg | 91.990(3) | 101.047(2) | 95.622(8) | 104.68(6) | | 90.99(5) | 112.54(2) | 114.220(3) |
| *γ*, deg | 101.947(4) | | | | | | | |
| *V*, Å$^3$ | 461.73(6) | 595.91(3) | 629.1(1) | 856.7(6) | 1684.9(2) | 914.9(7) | 914.7(3) | 1968.3(4) |
| *Z* | 1 | 2 | 2 | 2 | 4 | 2 | 2 | 4 |
| $\rho_{calc}$, g/cm$^3$ | 1.260 | 1.489 | 1.879 | 1.250 | 1.271 | 1.420 | 1.420 | 1.620 |
| $\mu$(Mo Kα), cm$^{-1}$ | 0.86 | 5.39 | 64.57 | 0.86 | 0.88 | 3.77 | 3.77 | 41.52 |
| $2\theta_{max}$, deg | 54.9 | 55.0 | 55.0 | 32.94 | 33.15 | 55.0 | 55.0 | 54.9 |
| diffractometer | RAXIS | RAXIS | RAXIS | DIP3000 | DIP3000 | AFC7R | AFC7R | RAXIS |
| reflections measured | 4045 | 5097 | 4523 | 2038 | 1792 | 2304 | 2339 | 4203 |
| unique reflections | 2043 | 1355 | 1394 | 2038 | 1765 | 2155 | 2093 | 2239 |
| $R_{merge}$ | 0.051 | 0.054 | 0.045 | 0.000 | | 0.031 | 0.036 | 0.066 |
| no. observed | 1429 | 1033 | 1141 | 1358 | 1111 | 965 | 1311 | 862 |
| | $I > 2\sigma(I)$ | $I > 2\sigma(I)$ | $I > 2\sigma(I)$ | $I > 3\sigma(I)$ | $I > 3\sigma(I)$ | $I > 2\sigma(I)$ | $I > 2\sigma(I)$ | $I > 2\sigma(I)$ |
| no. variables | 154 | 83 | 80 | 288 | 289 | 144 | 150 | 127 |
| parameter ratio | 9.28 | 12.45 | 14.26 | 4.72 | 3.84 | 6.70 | 8.74 | 6.79 |
| *R* | 0.082 | 0.058 | 0.041 | 0.039 | 0.039 | 0.069 | 0.042 | 0.083 |
| $R_w$ | 0.130 | 0.126 | 0.071 | 0.040 | 0.039 | 0.104 | 0.065 | 0.142 |
| GOF | 1.52 | 1.53 | 0.92 | 1.06 | 1.67 | 1.25 | 0.82 | 1.62 |
| temp, °C | 23 | −70 | 23 | 25 | 25 | −30 | −40 | 23 |
| final diff four map (e Å$^{-3}$) | 0.24, −0.28 | 0.64, −0.28 | 0.39, −0.77 | 0.11, −0.14 | 0.11, −0.15 | 0.60, −0.40 | 0.25, −0.40 | 0.79, −0.71 |

using a CCD camera system within a very short time, although they readily polymerized during the X-ray beam irradiation for the measurements using four-circle or imaging plate diffractometer systems.

Figure 4 shows the crystal structures of (*Z*,*Z*)-**4** and poly-((*Z*,*Z*)-**4**). The collection of the reflection data from the monomer crystal was carried out within 10 min to avoid the effect of the polymerization. The obtained crystal structure in the earliest

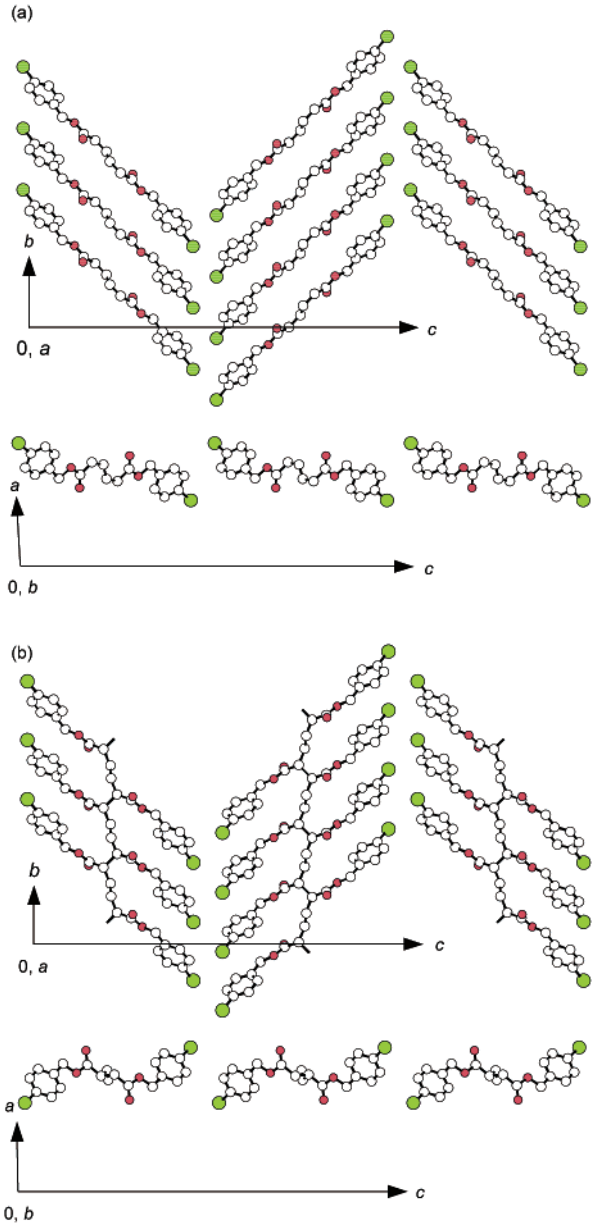


***Figure 4.*** Crystal structures of (a) (*Z*,*Z*)-**4** and (b) poly((*Z*,*Z*)-**4**): the view along the crystallographic *a* and *b* axes in top and bottom, respectively. Hydrogen atoms are omitted for clarity.

stage of the irradiation with the X-ray beams is regarded as that of the monomer. Crystals of both the monomer and polymer have identical space group and similar cell parameters: monoclinic, $P2_1/c$, $a = 5.629(6)$ Å, $b = 5.122(6)$ Å, $c = 32.08(2)$ Å, $\beta = 93.712(1)°$, $V = 923.0(4)$ Å$^3$, $Z = 2$ for the (*Z*,*Z*)-**4** monomer crystal, and monoclinic, $P2_1/c$, $a = 5.6796(3)$ Å, $b = 4.8631(1)$ Å, $c = 32.097(1)$ Å, $\beta = 90.185(2)°$, $V = 886.54(5)$ Å$^3$, $Z = 2$ for the poly((*Z*,*Z*)-**4**) crystal. Because the reflection from the monomer crystals observed at room temperature was somewhat insufficient for the least-squares refinement, the experiment was also carried out at −120 °C to successfully collect enough reflections without the effect of structural change as a result of the suppressed polymerization at a low temperature. The crystal structure at −120 °C agreed well with that at room temperature, except for a slight change in the lattice parameters dependent on the temperature: $a = 5.6457(2)$ Å, $b = 5.0639(3)$ Å, $c = 31.685(4)$ Å, $\beta = 92.746(4)°$, $V = 904.82(8)$ Å$^3$. The

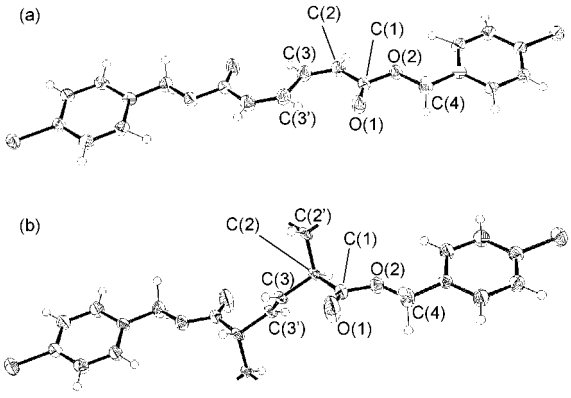


***Figure 5.*** ORTEP drawing for (*Z*,*Z*)-**4** (−120 °C) and repeating unit of poly((*Z*,*Z*)-**4**). Thermal ellipsoids are plotted at the 50% probability level.

successful determination of the crystal structure for the monomer and the polymer provides evidence for the topochemical polymerization process as well as the stereochemical structure of the polymer, that is, the *meso*-diisotactic-*trans*-2,5 structure.

In the monomer crystals, the monomer molecules stack along the *a* and *b* axes in a column structure. A polymer chain is assumed to be produced along the *b* axis from the consideration of the overlap of the $\pi$ orbitals of the reacting moieties, being in good agreement with the polymer crystal structure. The 4-chlorobenzyl moiety as the side chain has no significant change in its orientation during the polymerization. The polymerization proceeds with only rotation of the diene moiety and with no large movement of the center of mass. Figure 5 shows the ORTEP for (*Z*,*Z*)-**4** and poly((*Z*,*Z*)-**4**) that represents the precise molecular conformation. Selected geometry parameters are summarized in Table 4, together with the results for EMU and poly(EMU).[12b] The conformation of the main chain of poly((*Z*,*Z*)-**4**) is very similar to that of poly(EMU). These results indicate that the topochemical polymerization of (*Z*,*Z*)-**4** proceeds accompanying a change in the type of chemical bond with a minimum movement of atoms to produce a polymer chain in the crystals.

Figure 6 shows typical crystal structures for the monomers other than (*Z*,*Z*)-**4**. (*Z*,*Z*)-**6**-I has a crystal structure similar to that of (*Z*,*Z*)-**4**, but the molecular packing is completely different in another polymorph, (*Z*,*Z*)-**6**-II. The X-ray experiments at a lower temperature were also attempted for the (*Z*,*Z*)-**6**-I crystals, but they failed due to the difficulty in the single crystal structure fabrication at a low temperature and the phase transition of the monomer crystals. In most of the crystals examined in this study, monomer molecules favorably stack in a columnar structure when they have halogen-substituted ester groups, whereas no columnar structure was observed for the other crystals containing no halogen atoms.

## Discussion

**Monomer Stacking Distance and Polymerization Reactivity.** X-ray analysis has confirmed that all the muconate molecules have an *s*-trans conformation consisting of a highly planar structure, irrespective of the *EZ* configuration of the monomers. Most of them stack to give a columnar alignment. We have evaluated the packing structure of the monomer molecules in the crystals using four parameters, as shown in Figure 7, to discuss the relationship between the crystal structure

***Table 4.*** Selected Geometry Parameters for (*Z*,*Z*)-Muconate Monomers and Polymers

| | (*Z*,*Z*)-**4** | | | EMU[a] | |
|---|---|---|---|---|---|
| | monomer at r.t. | monomer at −120 °C | polymer | monomer | polymer |
| | | Intramolecular Bond Length (Å) | | | |
| C(1)−C(2) | 1.48(4) | 1.484(5) | 1.538(4) | 1.461(3) | 1.535(4) |
| C(2)−C(2′) | (3.56(3))[b] | (3.478(9))[b] | 1.564(5) | (3.791(3))[b] | 1.599(4) |
| C(2)−C(3) | 1.35(3) | 1.341(6) | 1.511(3) | 1.330(3) | 1.466(4) |
| C(3)−C(3′) | 1.47(3) | 1.469(8) | 1.322(5) | 1.428(3) | 1.309(3) |
| O(1)−C(1) | 1.19(4) | 1.212(4) | 1.190(5) | 1.196(3) | 1.194(3) |
| O(2)−C(4) | 1.42(3) | 1.449(4) | 1.435(3) | 1.458(3) | 1.71[c] |
| O(2)−C(1) | 1.34(4) | 1.353(5) | 1.329(3) | 1.335(3) | 1.296(3) |
| | | Intramolecular Bond Angles (deg) | | | |
| C(1)−C(2)−C(3) | 127.3(20) | 124.9(4) | 108.4(2) | 126.3(2) | 110.8(5) |
| C(1)−O(2)−C(4) | 110.2(18) | 115.2(3) | 117.0(2) | 116.3(2) | 117[c] |
| C(2)−C(3)−C(3′) | 128.1(18) | 126.6(5) | 123.5(3) | 127.1(2) | 125.4(4) |
| C(2)−C(1)−O(1) | 123.1(24) | 127.8(4) | 126.2(3) | 127.4(2) | 123.0(3) |
| C(2)−C(1)−O(2) | 108.2(22) | 109.0(3) | 109.9(3) | 109.9(2) | 111.3(4) |
| O(1)−C(1)−O(2) | 128.6(23) | 123.2(3) | 123.9(3) | 122.6(2) | 125.7(3) |
| | | Intramolecular Tortional Angles (deg) | | | |
| C(1)−C(2)−C(3)−C(3′) | −3.6(22) | 0.17[d] | 123.35[d] | −0.0(2) | 120.2(3) |
| C(4)−O(2)−C(1)−C(2) | 173.8(26) | −175.8(5) | 178.1(3) | −178.7(3) | −166[c] |
| O(1)−C(1)−C(2)−C(3) | −2.9(24) | 0.7(9) | 33.5(6) | −1.3(3) | 49.7(3) |
| O(2)−C(1)−C(2)−C(3) | −179.9(34) | −180.0(5) | −147.8(3) | −179.1(3) | −130.4(3) |

[a] Reference 13. [b] Intermolecular distance. [c] Their standard deviations are not described, since the C(4) atom is located in the abnormal position and has a large $U_{eq}$ value. [d] Standard deviations are not determined.

and the solid-state photopolymerization reactivity.[26] $\theta_1$ is the tilt angle viewed from direction I between the molecular plane and the column axis of the stacking molecules. Direction I is defined as that parallel to a vector through the intramolecular $C_2$ and $C_5$ carbons of the dienes. $\theta_2$ is another tilt angle viewed from direction II, which is orthogonally different from direction I. $d_{cc}$ is the intermolecular carbon-to-carbon distance between the $C_2$ and $C_5'$ carbons, which react to make a new bond during the topochemical polymerization. $d_s$ is the intermolecular stacking distance between the adjacent monomers in a column. The parameters determined for various muconate crystals are summarized in Table 5. In the previous papers, $\theta_1$ and $\theta_2$ were defined in an alternative way. Formerly, direction I was parallel to a vector through the 2- and 3-carbons (4- and 5-carbons) for the *Z*,*Z* monomers and through the 2- and 4-carbons (3- and 5-carbons) for the *E*,*E* monomers. Therefore, the values of $\theta_1$ and $\theta_2$ in this study are different from the previously reported values for some monomers.[13−16] The present method is better because of the unambiguousness and is valid even for nonplanar 1,3-butadiene derivatives.

The $d_s$ value of (*Z*,*Z*)-**6**-I was 5.21 Å, being slightly greater than that of (*Z*,*Z*)-**4** (5.06 and 5.12 Å at −120 °C and room temperature, respectively). The order in the $d_s$ values is related to the polymerization rate constant *k*; i.e., the larger the $d_s$ value, the slower the polymerization. The relatively large $d_s$ value is expected to induce any strain stored in the crystals during the polymerization. Actually, the single crystals of (*Z*,*Z*)-**6**-I are likely to have some damage, such as a crack or collapse during the photopolymerization. In contrast, the crystal structure of (*Z*,*Z*)-**4** is maintained during the polymerization as a result of the similar conformations in the monomer and polymer crystals (Figure 5 and Table 4) as well as the appropriate $d_s$ value. The $d_{cc}$ values for the methyl and decyl esters of the (*Z*,*Z*)- or (*E*,*E*)-muconates (3.55−3.79 Å) were almost the same as those for the polymerizable esters (3.48−3.89 Å), although they undergo no polymerization. The $\theta_1$ values for the photopolymerizable monomers are not distinguished from those for the nonpolymerizable one. In contrast, the experimental points are seen in a concentrated and specific region in the $d_s-\theta_2$ relationship in Figure 8; i.e., all the data points for the polymerizable monomers are situated in a limited range of 4.9−5.2 Å for $d_s$ and 43−55° for $\theta_2$. The curve in Figure 8 represents the calculated $d_s$ values for each $\theta_2$, assuming the closest packing of the molecular planes with a thickness of 3.5 Å and $\theta_1$ of 90°. A fiber period for the muconate polymers has been determined to be 4.8−4.9 Å in this and previous[12] studies, which is very close to the $d_s$ values for the polymerizable monomers. When the $d_s$ value agrees with the period of the repeating unit in the resulting polymer, the polymerization would successfully proceed.

Some halogenated benzyl esters have a smaller $d_s$ value than the unsubstituted or methyl-substituted benzyl esters (Table 5). It suggests that the ester monomer molecules can be more closely assembled by the introduction of a halogen atom to the phenyl ring. Interestingly, the $d_s$ values for nonpolymerizable (*Z*,*Z*)-**3** and (*Z*,*Z*)-**5** (4.04 and 4.11 Å, respectively) are smaller than those of the polymerizable monomers (vide infra). When the $\theta_2$ value is closer to 90°, there is a possibility for zigzag-type polymerization, which progresses with alternating $C_2-C_2'$ and $C_4-C_4'$ reaction. However, we observed no evidence for the polymerization of (*Z*,*Z*)-**3** and (*Z*,*Z*)-**5** during the photoirradiation. In other words, it is impossible to make a new carbon-to-carbon bond during the photoirradiation only by rotation of the diene moiety without any translational movement in the crystals when the $d_s$ value is shorter than the ideal one. It is concluded that the zigzag-type polymerization hardly occurs for the 1,3-diene monomers, although such a possibility was postulated for the diacetylene and diolefin polymerizations.[6f,27]

(26) Matsumoto, A.; Sada, K.; Tashiro, K.; Miyata, M.; Tsubouchi, T.; Tanaka, T.; Odani, T.; Nagahama, S.; Tanaka, T.; Inoue, K.; Saragai, S.; Nakamoto, S. *Angew. Chem., Int. Ed.*, in press.

(27) (a) Coates, G. W.; Dunn, A. R.; Henling, L. M.; Dougherty, D. A.; Grubbs, R. H. *Angew. Chem., Int. Ed*. **1997**, *36*, 248−251. (b) Coates, G. W.; Dunn, A. R.; Henling, L. M.; Ziller, J. W.; Lobkovsky, E. B.; Grubbs, R. H. *J. Am. Chem. Soc*. **1998**, *120*, 3641−3649.

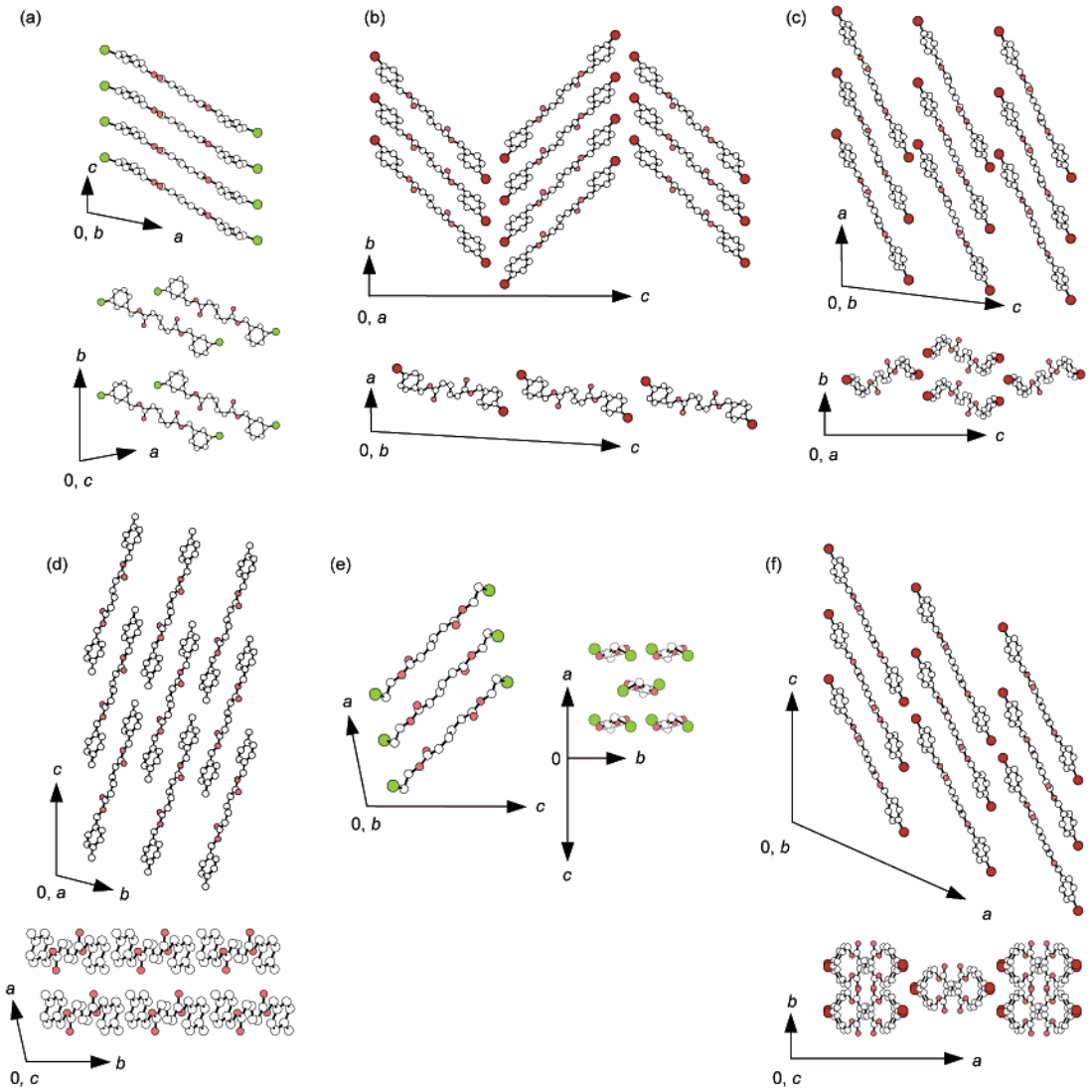


***Figure 6.*** Crystal structures of (a) (*Z*,*Z*)-**3**, (b) (*Z*,*Z*)-**6**-I, (c) (*Z*,*Z*)-**6**-II, (d) (*Z*,*Z*)-**7**, (e) (*Z*,*Z*)-**10**, and (f) (*E*,*E*)-**6**.

**Molecular Alignment with Weak Interactions between Halogen Atoms.** Figure 9 shows the halogen−halogen interaction observed in the crystals of (*Z*,*Z*)-**4**. From the viewpoint of intermolecular force for the monomer stacking, the following facts support the existence of a halogen−halogen interaction in the crystals of (*Z*,*Z*)-**4** and (*Z*,*Z*)-**6**-I. Initially, the distances between the nonbonding halogen atoms are 3.57 and 3.63 Å in the crystals of (*Z*,*Z*)-**4** and (*Z*,*Z*)-**6**-I, respectively, being shorter than the sum of the corresponding van der Waals radii. The distance between the nearest halogen atoms, $d_{x-x}$, is summarized in Table 6. Second, the Kitaigorodskii rule[1,8] breaks down for the benzyl muconates derivatives in this study, despite the validity of the rule for a large number of the other crystals of nonpolar and variously shaped aliphatic molecules. The substituent groups have no significant difference in their volumes (20 Å$^3$ for Cl, 26 Å$^3$ for Br, and 24 Å$^3$ for $CH_3$). The replacement of one by the other would not change their crystal structure when packing is governed by the Kitaigorodskii rule. Nevertheless, the crystal structure of 4-methyl-substituted (*Z*,*Z*)-**7** is completely different from those of the 4-chloro- and 4-bromo-substituted derivatives. The substitution for the chlorine atom by an electrically similar bromine atom does not alter the crystal structure; the monomer crystals of (*Z*,*Z*)-**4** and (*Z*,*Z*)-**6**-I belong to the same space groups and have lattice parameters that are similar to each other. In the crystal structure of (*Z*,*Z*)-**4** and (*Z*,*Z*)-**6**-I, the molecules are combined by the halogen zigzag chains (···X···X···X···, where X is Cl or Br) along the *b* axis through the halogen−halogen interaction to give a two-dimensional molecular sheet, implying a column structure in which the diene moieties are closely stacked (Figure 9a). This packing structure is favorable for the polymerization. These constructed molecular sheets are layered in the crystals, as shown by the three adjacent sheets viewed from the *b* axis. Such a structural motif with the halogen chain is also observed for the crystals of halogens,[24a] such as $Cl_2$,[28] $Br_2$,[29] and $I_2$.[30] The nearest distances of nonbonded halogen atoms are 3.27, 3.31, and 3.50 Å, respectively, to commonly form halogen zigzag chains along the *b* axis and a two-dimensional network sheet. This supports the fact that the alignment of the dibenzyl muconate monomers in the crystals is regulated by the characteristic halogen zigzag chains as a

(28) Stevens, E. D. *Mol. Phys.* **1979**, *37*, 27−45.
(29) Vonnegut, B.; Warren, B. E. *J. Am. Chem. Soc.* **1936**, *58*, 2459−2461.
(30) van Bolhuis, F. B.; Koster, P. B.; Migchlesan, T. *Acta Crystallogr.* **1967**, *23*, 90−91.

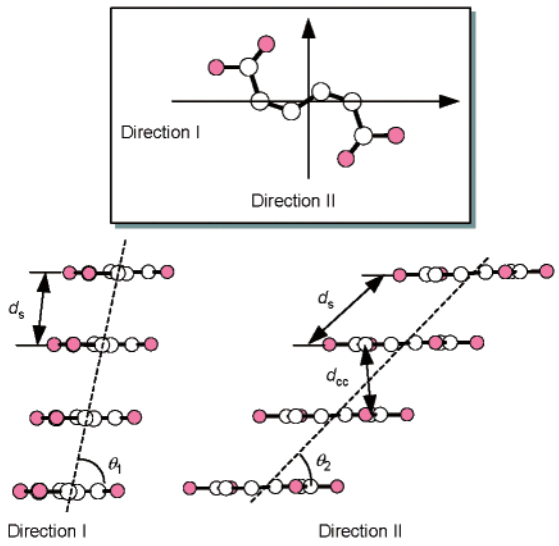


***Figure 7.*** Stacking model for the muconate derivatives in the crystalline state and the definition of stacking parameters used for the prediction of the topochemical polymerization reactivity. $d_{cc}$ is the intermolecular distance between the 2- and 5′-carbons; $d_s$ is the stacking distance between the adjacent monomers in a column; $\theta_1$ and $\theta_2$ are the angles between the stacking direction and the molecular plane in orthogonally different directions. The view from direction I is parallel to a vector through the 2- and 5-carbons of the diene moieties.

***Table 5.*** Stacking Parameters for Crystals of Various Muconates[a]

| monomer | $d_{cc}$ (Å) | $d_s$ (Å) | $\theta_1$ (deg) | $\theta_2$ (deg) | ref[b] |
|---|---|---|---|---|---|
| Topochemically Polymerizable Monomers | | | | | |
| (*Z*,*Z*)-**4** (r.t.) | 3.56 | 5.12 | 82 | 44 | this work |
| (*Z*,*Z*)-**4** (−120 °C) | 3.48 | 5.06 | 78 | 43 | this work |
| (*Z*,*Z*)-**6**-I | 3.89 | 5.21 | 72 | 49 | this work |
| EMU (r.t.) | 3.79 | 4.93 | 79 | 49 | 12b |
| (*Z*,*Z*)-BnAm[c] | 4.24 | 4.86 | 67 | 55 | 15a |
| (*Z*,*Z*)-2ClBnAm[d] | 4.19 | 4.94 | 62 | 52 | 15a |
| Topochemically Nonpolymerizable Monomers | | | | | |
| (*Z*,*Z*)-**1**-I | 6.42 | 5.69 | 12 | 61 | 13 |
| (*Z*,*Z*)-**1**-II | 6.14 | 9.37 | 52 | 19 | this work |
| (*Z*,*Z*)-**3** | 4.35 | 4.04 | 67 | 67 | this work |
| (*Z*,*Z*)-**5** | 5.17 | 4.11 | 66 | 82 | this work |
| (*Z*,*Z*)-**6**-II | 5.01 | 8.05 | 62 | 24 | this work |
| (*Z*,*Z*)-**7** | 8.55 | 11.72 | 49 | 19 | this work |
| (*Z*,*Z*)-**10** | 4.92 | 5.42 | 16 | 26 | this work |
| (*Z*,*Z*)-**11** | 5.00 | 5.50 | 17 | 27 | this work |
| (*Z*,*Z*)-**12** | 4.02 | 5.86 | 68 | 40 | 13 |
| (*Z*,*Z*)-methyl | 3.79 | 5.79 | 72 | 39 | 13 |
| EMU (−80 °C)[e] | 3.88 | 4.25 | 80 | 57 | 14 |
| (*Z*,*Z*)-decyl | 3.69 | 5.50 | 70 | 40 | 13 |
| (*Z*,*Z*)-cyclohexyl | 5.20 | 6.93 | 32 | 28 | 13 |
| (*E*,*E*)-**1**-I | 5.91 | 5.71 | 6 | 20 | this work |
| (*E*,*E*)-**1**-II | 5.88 | 5.77 | 6 | 20 | this work |
| (*E*,*E*)-**2** | 4.22 | 6.02 | 58 | 39 | this work |
| (*E*,*E*)-**3** | 5.99 | 9.37 | 83 | 18 | this work |
| (*E*,*E*)-**6** | 5.98 | 5.67 | 1 | 4 | this work |
| (*E*,*E*)-**12** | 4.51 | 6.07 | 41 | 36 | 13 |
| (*E*,*E*)-methyl | 3.55 | 5.81 | 63 | 33 | 13 |
| (*E*,*E*)-ethyl | 5.44 | 7.85 | 45 | 29 | 13 |
| (*E*,*E*)-cyclohexyl | 6.76 | 9.37 | 76 | 25 | 13 |

[a] $d_{cc}$, distance between the reacting $C_2$ and $C_5'$ carbons; $d_s$, stacking distance; $\theta_1$, $\theta_2$, tilt angles of the molecular plane. [b] References to crystal structure. [c] Di(benzylammonium) (*Z*,*Z*)-muconate. [d] Di(2-chlorobenzylammonium) (*Z*,*Z*)-muconate. [e] Low-temperature phase.

supramolecular synthon, which may be applicable for the crystal design of halogen-containing ester derivatives.

The selection of halogen atoms as well as the position of substitution may be important for crystal designs based on

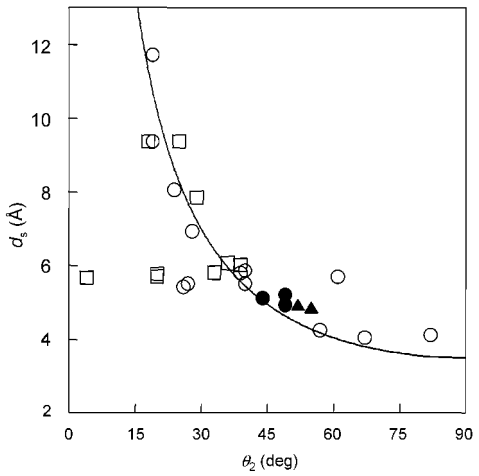


***Figure 8.*** Relationship between $\theta_2$ and $d_s$. The curve is the calculated $d_s$ values for the closed packing in the column, assuming a molecular thickness of 3.5 Å and $\theta_2$ of 90°: (●) polymerizable (*Z*,*Z*)-muconic esters, (▲) polymerizable (*Z*,*Z*)-muconic ammonium salts, (○) nonpolymerizable (*Z*,*Z*)-muconic esters, and (□) nonpolymerizable (*E*,*E*)-muconic esters.

halogen−halogen interaction. In contrast to the 4-chloro and bromo derivatives, (*Z*,*Z*)-**5** does not form such a halogen chain because of a weak interaction between the fluorine atoms. The case of the (*Z*,*Z*)-**3** crystal suggests that the substitution position may play an important role in determining the pattern of the halogen interaction in the crystals. These monomers produced an aromatic stack of the benzyl groups characterized by a short stacking distance, that is, 4.11 and 4.04 Å in the crystals of (*Z*,*Z*)-**5** and (*Z*,*Z*)-**3**, respectively. As the actual structure, a stacking column in the crystal of (*Z*,*Z*)-**5** is shown in Figure 10. A similar stacking mode with nearly the same stacking distance is commonly seen in a large number of crystals for other halogenated aromatic compounds.[1,32] The resulting $d_s$ values are too short to be suitable for photopolymerization. Being different from the aspect of the derivatives described above, (*E*,*E*)-**2**, (*E*,*E*)-**3**, and (*E*,*E*)-**6** form neither the halogen zigzag chain nor the stacked structure of halogenated aromatics, despite the interaction between the nearest halogen atoms. This is attributed to a delicate balance of many energy terms associated with the closed packing and halogen−halogen interaction.

The halogen-substituted ethyl esters, (*Z*,*Z*)-**10** and (*Z*,*Z*)-**11**, form no zigzag chain structure, although the halogen atoms closely contact each other in these crystals. It supports the role of the aromatic rings for the columnar alignment. In the crystals of (*Z*,*Z*)-**4** and (*Z*,*Z*)-**6**-I, CH/$\pi$ interactions between the benzylic hydrogen atom and the aromatic ring are also observed (Figure 9c). The molecules are connected by a CH/$\pi$ interaction as well as halogen chains to strengthen the columnar structure appropriate for the polymerization. Table 6 also summarizes the closest $C(sp_2)$−HC contacts for structural units regarding the CH/$\pi$ interaction. The C−H distance for the close contacts between the aromatic rings and benzylic hydrogen is 3.11 and 2.98 Å, for (*Z*,*Z*)-**4** and (*Z*,*Z*)-**6**-I, respectively. The CH/$\pi$ interaction is also found in the crystal of the nonsubstituted benzyl ester, where the aromatic and benzylic hydrogens result in a compli-

(31) (a) Johdan, T. H.; Streib, W. E.; Lipscomb, W. N. *J. Chem. Phys.* **1964**, *41*, 760−764. (b) Meyer, L.; Barrett, C. S.; Greer, S. C. *J. Chem. Phys.* **1968**, *49*, 1902−1907.
(32) Sarma, J. A. R. P.; Desiraju, G. R. *Acc. Chem. Res.* **1986**, *19*, 222−228.

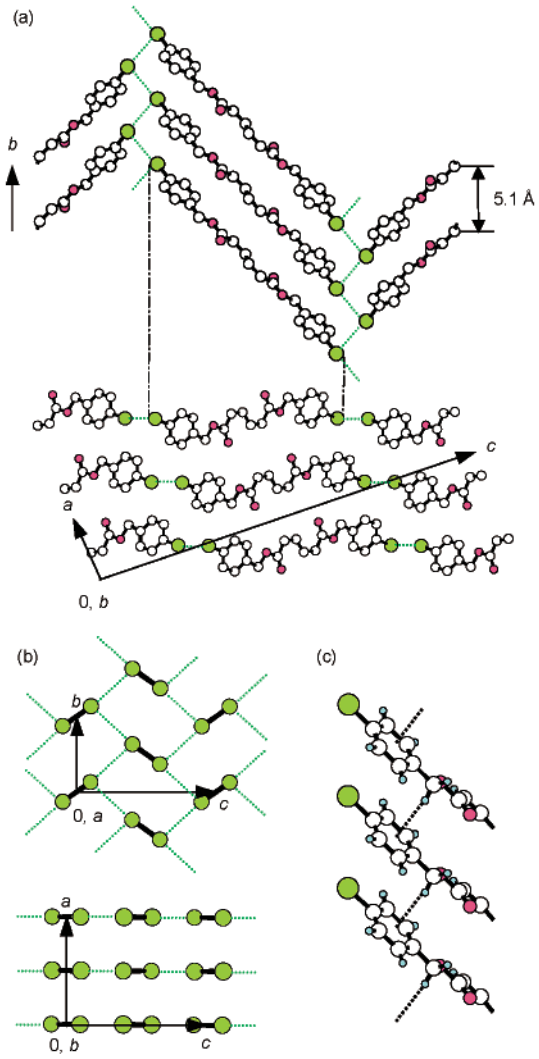


***Figure 9.*** (a) Molecular sheet with halogen zigzag chain (top) and the three adjacent sheets viewed along the crystallographic *b* axis (bottom) in the crystal of (*Z*,*Z*)-**4**. (b) The crystal structure of $Cl_2$ is shown in a similar manner as (*Z*,*Z*)-**4**. Dotted lines show halogen−halogen interactions. (c) CH/$\pi$ interaction in the crystals of (*Z*,*Z*)-**4**.

cated structure but not a column structure in the crystals of (*Z*,*Z*)-**1**. The 1-naphthylmethyl ester, (*Z*,*Z*)-**8**, also seems to be similar to the benzyl ester. Although CH/$\pi$ and halogen−halogen interactions are seen in the crystals of the monomers involving an aromatic ring and halogen atom, respectively, only when both of the interactions simultaneously function in a columnar alignment suitable for the polymerization constructed in the crystals. Thus, the control of the molecular alignment through a halogen−halogen interaction is effective in combination with any other weak interaction.

**Conclusions.** We have found that topochemical polymerization is efficiently induced by the substitution of an aromatic hydrogen for an halogen atom in the benzyl ester of (*Z*,*Z*)-muconic acid, whereas a number of alkyl muconates and unsubstituted or alkylated benzyl muconates are nonpolymerizable. X-ray single crystal structure analysis of the monomer and polymer crystals has confirmed the topochemical polymerization process via a crystal-to-crystal reaction mechanism. In a large number of muconate crystals, monomer molecules favorably form a columnar alignment of conjugated diene moieties. The stacking distance of the monomers determines

***Table 6.*** Non-Bonding Halogen Atoms and C($sp_2$)−HC Contacts in the Muconate Crystals

| | halogen−halogen | | CH/$\pi$ | | |
|---|---|---|---|---|---|
| monomer | contacts | $d_{x-x}$ (Å)[a] | contacts[b] | $d_{C(sp2)-H}$ (Å) | ref |
| (*Z*,*Z*)-**1**-I | | | ArH−Ar | 2.81 | 13 |
| (*Z*,*Z*)-**1**-II | | | BnH−Ar | 2.95 | 13 |
| (*Z*,*Z*)-**3** | Cl···Cl | (4.04) | | | this work |
| (*Z*,*Z*)-**4** (r.t.) | Cl···Cl | 3.57 | BnH−Ar | 3.11 | this work |
| (*Z*,*Z*)-**4** (−120 °C) | Cl···Cl | 3.50 | BnH−Ar | 3.07 | this work |
| poly((*Z*,*Z*)-**4**) | Cl···Cl | 3.54 | BnH−Ar | 2.87 | this work |
| (*Z*,*Z*)-**5** | F···F | (3.14) | | | this work |
| (*Z*,*Z*)-**6**-I | Br···Br | 3.63 | BnH−Ar | 2.98 | this work |
| (*Z*,*Z*)-**6**-II | Br···Br | 3.53 | | | this work |
| (*Z*,*Z*)-**10** | Cl···Cl | 3.32 | | | this work |
| (*Z*,*Z*)-**11** | Br···Br | 3.82 | | | this work |
| (*Z*,*Z*)-**12** | Cl···Cl | (3.92) | | | 13 |
| (*E*,*E*)-**2** | Cl···Cl | (3.88) | | | this work |
| (*E*,*E*)-**3** | Cl···Cl | 3.56 | | | this work |
| (*E*,*E*)-**6** | Br···Br | 3.59 | ArH−Ar | 2.96 | this work |
| (*E*,*E*)-**12** | Cl···Cl | 3.11 | | | 13 |
| $F_2$ | F···F | (2.88) | | | 31 |
| $Cl_2$ | Cl···Cl | 3.27 | | | 28 |
| $Br_2$ | Br···Br | 3.31 | | | 29 |

[a] $d_{x-x}$ is the closest distance between nonbonding halogen atoms. $d_{C(sp_2)-HC}$ is the closest distance between the aromatic carbon atom and the hydrogen atom located above the aromatic ring. The values in parentheses are greater than the sum of the corresponding van der Waals radii. [b] ArH−Ar: contact between aromatic hydrogen and aromatic ring. BnH−Ar: contact between benzylic hydrogen and aromatic ring.

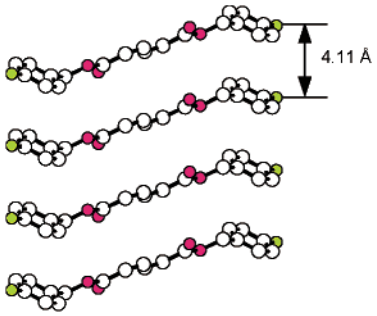


***Figure 10.*** Monomer stacking structure in the (*Z*,*Z*)-**5** crystal. The stacking distance is 4.11 Å, but this monomer is nonpolymerizable.

the polymerization reactivity in the crystalline state, and the polymerization proceeds when the stacking distance is 5 Å. The monomers are connected through two intermolecular interactions, such as a halogen−halogen and CH/$\pi$ interaction to provide and strengthen the columnar alignment of the diene moieties suitable for polymerization, as seen in the crystals of (*Z*,*Z*)-**4** and (*Z*,*Z*)-**6**-I.

The control of the molecular alignment through a halogen−halogen interaction is effective only in the absence of a more robust interaction, such as hydrogen bonding. For example, the crystal of benzylammonium (*Z*,*Z*)-muconate, which has a robust two-dimensional hydrogen-bonded network, is not disturbed by the introduction of halogen atoms into the aromatic ring.[15a] Thus, the halogen−halogen interaction as supramolecular synthons has a significant potential in the presence of other weak interactions and is used for rational crystal design of the diene monomers other than the ammonium derivatives. More recently, we have already found that the combination of the CH/$\pi$ interaction with the C−H···O interaction is useful for the design of the topochemical polymerization to yield a new type of stereoregular polymer. These results will be separately reported in the near future.

## Experimental Section

**General Methods.** NMR, IR, and UV spectra were recorded on a JEOL JMN A-400, JASCO Herschel FT-IR-430, and Shimadzu UV-160 spectrometer, respectively. The powder X-ray diffraction profile was recorded on Shimadzu XD-610 or Rigaku RINT-2100 with monochromatized Cu Kα radiation ($\lambda = 1.54118$ Å).

**Materials.** (*Z*,*Z*)-Muconic acid, supplied from Mitsubishi Chemical Co., Ltd., Tokyo, was used without any further purification. All of the esters were prepared by the reaction of the (*Z*,*Z*)-muconic acid with thionyl chloride, followed by esterification with the corresponding alcohols.

(*Z*,*Z*)-Muconic acid dichloride was obtained from (*Z*,*Z*)-muconic acid (1.42 g) with thionyl chloride (1.5 mL) in the presence of a drop of *N*,*N*-dimethylformamide in 50 mL of dichloromethane with reflux for 5 h. The obtained acid chloride was added dropwise with stirring at 0 °C to a dichloromethane solution (50 mL) containing 2.85 g of 2-chlorobenzyl alcohol and 1.5 mL of triethylamine. After further stirring at room temperature for 1 day, the solvent was evaporated. The product was purified by silica gel column chromatography with 1,2-dichloroethane, followed by recrystallization from chloroform to provide needles with a melting point of 75.1−75.7 °C. The isolated yield of (*Z*,*Z*)-**2** was 10%.

The corresponding *E*,*E* isomer ((*E*,*E*)-**2**) was simultaneously obtained from the reaction mixture by column chromatography. When it was contaminated with the *E*,*Z* isomer, they were isolated as the pure *E*,*E* isomer after isomerization by heating. (*E*,*E*)-**2** was recrystallized from chloroform: Prisms, mp 99.4−102.3 °C. The *E*,*E* monomers were also prepared by an alternative and direct method. The refluxing of (*Z*,*Z*)-muconic acid and thionyl chloride in 1,2-dichloroethane in the presence of pyridine provided (*E*,*E*)-muconic acid dichloride, but not as a mixture of the isomers of the muconic acid dichloride.

Spectral data for the *Z*,*Z* and *E*,*E* derivatives are as follows:

Di(2-chlorobenzyl) (*Z*,*Z*)-muconate ((*Z*,*Z*)-**2**): Needles, mp 75.1−75.7 °C ($CHCl_3$) for (*Z*,*Z*)-**2**-I; needles, mp 75.7−76.1 °C ($CHCl_3$) for (*Z*,*Z*)-**2**-II; $^1$H NMR (400 MHz, $CDCl_3$) $\delta$ 7.96 (m, C*H*═$CHCO_2$R, 2H), 7.26−7.44 (m, $C_6H_4$, 8H), 6.07 (m, CH═C*H*$CO_2$R, 2H), 5.30 (s, $OCH_2$, 4H); $^{13}$C NMR (100 MHz, $CDCl_3$) $\delta$ 165.17 (C═O), 138.55 (CH═), 133.74, 133.33, 129.96, 129.63, 126.93, and 123.88 ($C_6H_4$ and CH═), 63.65 ($OCH_2$); UV (acetonitrile) $\lambda_{max}$ 262 nm ($\epsilon = 27\,600$).

Di(3-chlorobenzyl) (*Z*,*Z*)-muconate ((*Z*,*Z*)-**3**): Needles, mp 100.8−101.1 °C, ($CHCl_3$); $^1$H NMR (400 MHz, $CDCl_3$) $\delta$ 7.94 (m, C*H*═$CHCO_2$R, 2H), 7.25−7.37 (m, $C_6H_4$, 8H), 6.05 (m, CH═C*H*$CO_2$R, 2H), 5.16 (s, $OCH_2$, 4H); $^{13}$C NMR (100 MHz, $CDCl_3$) $\delta$ 165.14 (C═O), 138.61 (CH═), 137.62, 134.48, 129.91, 128.49, 128.23, 126.20, and 123.85 ($C_6H_4$ and CH═), 65.37 ($OCH_2$); UV (acetonitrile) $\lambda_{max}$ 260 nm ($\epsilon = 26\,900$).

Di(4-chlorobenzyl) (*Z*,*Z*)-muconate ((*Z*,*Z*)-**4**): Plates, mp 130.8−131.0 °C ($CHCl_3$); $^1$H NMR (400 MHz, $CDCl_3$) $\delta$ 7.91 (m, C*H*═$CHCO_2$R, 2H), 7.32 (m, $C_6H_4$, 8H), 6.01 (m, CH═C*H*$CO_2$R, 2H), 5.14 (s, $OCH_2$, 4H); $^{13}$C NMR (100 MHz, $CDCl_3$) $\delta$ 165.15 (C═O), 138.46 (CH═), 134.21, 134.15, 129.62, 128.77, and 123.86 ($C_6H_4$ and CH═), 65.42 ($OCH_2$); IR (KBr) 1712 ($\nu_{C=O}$), 1588 ($\nu_{C=C}$), 754 ($\nu_{C=C}$) $cm^{-1}$; UV (acetonitrile) $\lambda_{max}$ 261 nm ($\epsilon = 24\,300$).

Di(4-fluorobenzyl) (*Z*,*Z*)-muconate ((*Z*,*Z*)-**5**): Plates, mp 113.6−113.9 °C ($CHCl_3$); $^1$H NMR (400 MHz, $CDCl_3$) $\delta$ 7.91 (m, C*H*═$CHCO_2$R, 2H), 7.20 (m, $C_6H_4$, 8H), 6.01 (m, CH═C*H*$CO_2$R, 2H), 5.15 (s, $OCH_2$, 4H); $^{13}$C NMR (100 MHz, $CDCl_3$) $\delta$ 165.28 (C═O), 161.45 ($C_6H_4$), 138.43 (CH═), 131.47, 130.37, 123.95, and 115.44 ($C_6H_4$ and CH═), 65.59 ($OCH_2$); UV (methanol) $\lambda_{max}$ 262 nm ($\epsilon = 28\,600$).

Di(4-bromobenzyl) (*Z*,*Z*)-muconate ((*Z*,*Z*)-**6**): Plates, mp 142.0−142.4 °C ($CHCl_3$) for (*Z*,*Z*)-**6**-I; Prisms, mp 142.2−143.1 °C ($CHCl_3$) for (*Z*,*Z*)-**6**-II; $^1$H NMR (400 MHz, $CDCl_3$) $\delta$ 7.91 (m, C*H*═$CHCO_2$R, 2H), 7.37 (m, $C_6H_4$, 8H), 6.02 (m, CH═C*H*$CO_2$R, 2H), 5.13 (s, $OCH_2$, 4H); $^{13}$C NMR (100 MHz, $CDCl_3$) $\delta$ 165.15 (C═O), 138.49 (CH═), 134.67, 131.74, 129.92, 122.40, and 123.86 ($C_6H_4$ and CH═), 65.47 ($OCH_2$); UV (acetonitrile) $\lambda_{max}$ 260 nm ($\epsilon = 26\,100$).

Di(4-methylbenzyl) (*Z*,*Z*)-muconate ((*Z*,*Z*)-**7**): Prisms, mp 103.5−103.6 °C ($CHCl_3$); $^1$H NMR (400 MHz, $CDCl_3$) $\delta$ 7.91 (m, C*H*═$CHCO_2$R, 2H), 7.21 (m, $C_6H_4$, 8H), 6.00 (m, CH═C*H*$CO_2$R, 2H), 5.14 (s, $OCH_2$, 4H), 2.35 (s, $CH_3$, 6H); $^{13}$C NMR (100 MHz, $CDCl_3$) $\delta$ 165.45 (C═O), 138.27 (CH═), 132.66, 129.30, 128.48, and 124.08 ($C_6H_4$ and CH═), 66.68 ($OCH_2$), 21.23 ($CH_3$); UV (methanol) $\lambda_{max}$ 262 nm ($\epsilon = 28\,600$).

Di(1-naphthylmethyl) (*Z*,*Z*)-muconate ((*Z*,*Z*)-**8**): Plates, mp 122.0−122.2 °C ($CHCl_3$); $^1$H NMR (400 MHz, $CDCl_3$) $\delta$ 7.43−8.03 (m, C*H*═$CHCO_2$R and $C_{10}H_7$, 16H), 6.00 (m, CH═C*H*$CO_2$R, 2H), 5.64 (d, $J = 3.2$ Hz, $OCH_2$, 4H); $^{13}$C NMR (100 MHz, $CDCl_3$) $\delta$ 165.45 (C═O), 138.41 (CH═), 133.74, 131.62, 131.14, 129.48, 128.77, 127.70, 126.65, 126.02, 125.30, 124.01, and 123.54 ($C_{10}H_7$ and CH═), 64.65 ($OCH_2$); UV (acetonitrile) $\lambda_{max}$ 222 nm ($\epsilon = 165\,100$).

Di(2-naphthylmethyl) (*Z*,*Z*)-muconate ((*Z*,*Z*)-**9**): Powder, mp 157.7−158.1 °C ($CHCl_3$); $^1$H NMR (400 MHz, $CDCl_3$) $\delta$ 7.96 (m, C*H*═$CHCO_2$R, 2H), 7.45−7.85 (m, $C_{10}H_7$, 14H), 6.06 (m, CH═C*H*$CO_2$R, 2H), 5.34 (s, $OCH_2$, 4H); $^{13}$C NMR (100 MHz, $CDCl_3$) $\delta$ 165.42 (C═O), 138.45 (CH═), 133.16, 133.13, 133.06, 128.46, 128.00, 127.90, 127.72, 127.47, 126.35, 125.88, and 124.07 ($C_{10}H_7$ and CH═), 66.48 ($OCH_2$); UV (acetonitrile) $\lambda_{max}$ 223 nm ($\epsilon = 71\,000$).

Di(2-chloroethyl) (*Z*,*Z*)-muconate ((*Z*,*Z*)-**10**): Plates, mp 104.1−105.0 °C; $^1$H NMR (400 MHz, $CDCl_3$) $\delta$ 7.92 (m, C*H*═$CHCO_2$R, 2H), 6.04 (m, CH═C*H*$CO_2$R, 2H), 4.42 (t, $J = 6.0$ Hz, $OCH_2$, 4H); 3.73 (t, $J = 6.0$ Hz, $CH_2Cl$, 4H); $^{13}$C NMR (100 MHz, $CDCl_3$) $\delta$ 164.98 (C═O), 138.56 and 123.71 (CH═), 64.02 ($OCH_2$), 41.41 ($CH_2Cl$); UV (acetonitrile) $\lambda_{max}$ 260 nm ($\epsilon = 21\,600$).

Di(2-bromoethyl) (*Z*,*Z*)-muconate ((*Z*,*Z*)-**11**): Plates, mp 97.1− 98.2 °C; $^1$H NMR (400 MHz, $CDCl_3$) $\delta$ 7.94 (m, C*H*═$CHCO_2$R, 2H), 6.04 (m, CH═C*H*$CO_2$R, 2H), 4.48 (t, $J = 6.0$ Hz, $OCH_2$, 4H); 3.56 (t, $J = 6.0$ Hz, $CH_2Cl$, 4H); $^{13}$C NMR (100 MHz, $CDCl_3$) $\delta$ 164.92 (C═O), 138.64 and 123.73 (CH═), 63.84 ($OCH_2$), 28.48 ($CH_2Cl$); UV (acetonitrile) $\lambda_{max}$ 260 nm ($\epsilon = 20\,600$).

Bis(2,2,2-trichloroethyl) (*Z*,*Z*)-muconate ((*Z*,*Z*)-**12**): Plates, mp 124.3−125.2 °C; $^1$H NMR (400 MHz, $CDCl_3$) $\delta$ 8.02 (m, C*H*═$CHCO_2$R, 2H), 6.17 (m, CH═C*H*$CO_2$R, 2H), 4.83 (t, $J = 6.0$ Hz, $OCH_2$, 4H); $^{13}$C NMR (100 MHz, $CDCl_3$) $\delta$ 163.52 (C═O), 139.53 and 123.34 (CH═), 94.67 ($CCl_3$), 74.02 ($OCH_2$); UV (acetonitrile) $\lambda_{max}$ 263 nm ($\epsilon = 21\,200$).

Di(2-chlorobenzyl) (*E*,*E*)-muconate ((*E*,*E*)-**2**): Prisms, mp 99.4−102.3 °C ($CHCl_3$); $^1$H NMR (400 MHz, $CDCl_3$) $\delta$ 7.96 (m, C*H*═$CHCO_2$R, 2H), 7.26−7.44 (m, $C_6H_4$, 8H), 6.07 (m, CH═C*H*$CO_2$R, 2H), 5.30 (s, $OCH_2$, 4H); $^{13}$C NMR (100 MHz, $CDCl_3$) $\delta$ 165.46 (C═O), 141.38 (CH═), 133.82, 133.26, 129.99, 129.71, 129.66, 128.10, and 126.93 ($C_6H_4$ and CH═), 64.06 ($OCH_2$); UV (acetonitrile) $\lambda_{max}$ 265 nm ($\epsilon = 34\,500$).

Di(3-chlorobenzyl) (*E*,*E*)-muconate ((*E*,*E*)-**3**): Prisms, mp 101.9−102.6 °C ($CHCl_3$); $^1$H NMR (400 MHz, $CDCl_3$) $\delta$ 7.25−7.38 (m, C*H*═$CHCO_2$R and $C_6H_4$, 10H), 6.27 (m, CH═C*H*$CO_2$R, 2H), 5.18 (s, $OCH_2$, 4H); $^{13}$C NMR (100 MHz, $CDCl_3$) $\delta$ 165.45 (C═O), 141.38 (CH═), 137.53, 134.50, 129.92, 128.56, 128.28, 128.10, and 126.27 ($C_6H_4$ and CH═), 65.77 ($OCH_2$); UV (acetonitrile) $\lambda_{max}$ 266 nm ($\epsilon = 34\,700$).

Di(4-chlorobenzyl) (*E*,*E*)-muconate ((*E*,*E*)-**4**): Powder, mp 153.6−156.8 °C ($CHCl_3$); $^1$H NMR (400 MHz, $CDCl_3$) $\delta$ 7.27−7.36 (m, C*H*═$CHCO_2$R and $C_6H_4$, 10H), 6.24 (m, CH═C*H*$CO_2$R, 2H), 5.18 (s, $OCH_2$, 4H); $^{13}$C NMR (100 MHz, $CDCl_3$) $\delta$ 165.50 (C═O), 141.29 (CH═), 134.35, 129.74, 128.82, 128.13, and 123.88 ($C_6H_4$ and CH═), 65.88 ($OCH_2$); UV (acetonitrile) $\lambda_{max}$ 265 nm ($\epsilon = 30\,900$).

Di(4-fluorobenzyl) (*E*,*E*)-muconate ((*E*,*E*)-**5**): Powder, mp 113.4−114.1 °C ($CHCl_3$); $^1$H NMR (400 MHz, $CDCl_3$) $\delta$ 7.03−7.38 (m, C*H*═$CHCO_2$R and $C_6H_4$, 10H), 6.23 (m, CH═C*H*$CO_2$R, 2H), 5.18 (s, $OCH_2$, 4H); $^{13}$C NMR (100 MHz, $CDCl_3$) $\delta$ 165.58 (C═O), 161.45

($C_6H_4$), 141.23 (CH═), 131.57, 130.45, 128.18, and 115.69 ($C_6H_4$ and CH═), 66.00 ($OCH_2$); UV (methanol) $\lambda_{max}$ 265 nm ($\epsilon$ = 30 000).

Di(4-bromobenzyl) (*E*,*E*)-muconate ((*E*,*E*)-**6**): Prisms, mp 143.1−147.4 °C ($CHCl_3$); $^1$H NMR (400 MHz, $CDCl_3$) $\delta$ 7.38 (m, $C_6H_4$, 8H), 7.33 (m, C*H*═CHCO$_2$R, 2H), 6.23 (m, CH═C*H*CO$_2$R, 2H), 5.16 (s, $OCH_2$, 4H); $^{13}$C NMR (100 MHz, $CDCl_3$) $\delta$ 165.48 (C═O), 141.31 (CH═), 134.55, 131.78, 130.2, 128.11, and 122.50 ($C_6H_4$ and CH═), 65.92 ($OCH_2$); UV (acetonitrile) $\lambda_{max}$ 265 nm ($\epsilon$ = 35 300).

Di(4-methylbenzyl) (*E*,*E*)-muconate ((*E*,*E*)-**7**): Needles, mp 132.1−135.7 °C ($CHCl_3$); $^1$H NMR (400 MHz, $CDCl_3$) $\delta$ 7.32 (m, C*H*═CHCO$_2$R, 2H), 7.22 (m, $C_6H_4$, 8H), 6.21 (m, CH═C*H*CO$_2$R, 2H), 5.17 (s, $OCH_2$, 4H), 2.35 (s, $CH_3$, 6H); $^{13}$C NMR (100 MHz, $CDCl_3$) $\delta$ 165.73 (C═O), 141.11 (CH═), 138.33, 132.56, 129.30, 128.56, and 128.24 ($C_6H_4$ and CH═), 66.67 ($OCH_2$), 21.18 ($CH_3$); UV (acetonitrile) $\lambda_{max}$ 265 nm ($\epsilon$ = 34 000).

Di(1-naphthylmethyl) (*E*,*E*)-muconate ((*E*,*E*)-**8**): Powder, mp 164.3−164.9 °C ($CHCl_3$); $^1$H NMR (400 MHz, $CDCl_3$) $\delta$ 7.43−8.01 (m, $C_{10}H_7$, 14H), 7.30 (m, C*H*═CHCO$_2$R, 2H), 6.21 (m, CH═C*H*CO$_2$R, 2H), 5.66 (s, $OCH_2$, 4H); $^{13}$C NMR (100 MHz, $CDCl_3$) $\delta$ 165.71 (C═O), 141.24 (CH═), 133.71, 131.62, 131.04, 129.51, 128.75, 128.21, 127.72, 126.67, 126.02, 125.27, and 123.49 ($C_{10}H_7$ and CH═), 65.03 ($OCH_2$); UV (acetonitrile) $\lambda_{max}$ 221 nm ($\epsilon$ = 134 400).

Di(2-naphthylmethyl) (*E*,*E*)-muconate ((*E*,*E*)-**9**): Plates, mp 181.8−182.4 °C ($CHCl_3$); $^1$H NMR ((400 MHz, $CDCl_3$) $\delta$ 7.81−7.87 (m, $C_{10}H_7$, 8H), 7.45−7.53 (m, $C_{10}H_7$, 6H), 7.37 (m, C*H*═CHCO$_2$R, 2H), 6.27 (m, CH═C*H*CO$_2$R, 2H), 5.38 (s, $OCH_2$, 4H); $^{13}$C NMR (100 MHz, $CDCl_3$) $\delta$ 165.71 (C═O), 141.26 (CH═), 133.15, 132.95, 129.54, 128.47, 128.09, 128.00, 127.72, 127.57, 126.38, and 125.91 ($C_{10}H_7$ and CH═), 66.88 ($OCH_2$); UV (acetonitrile) $\lambda_{max}$ 223 nm ($\epsilon$ = 80 000).

**Photoreaction.** The monomer crystals were photoirradiated with a high-pressure mercury lamp (Toshiba SHL-100-2, 100 W, Pyrex filter) at a distance of 10 or 20 cm under atmospheric conditions at room temperature. After irradiation, the polymers were isolated by removal of the unreacted monomer with chloroform. The polymer yield was gravimetrically determined. The isomer composition of the recovered monomers was determined by $^1$H NMR spectroscopy. For fabrication of the polymer single crystals of (*Z*,*Z*)-**4**, the monomer single crystals were cut in an appropriate size and charged in a Pyrex tube, degassed, and then sealed. $\gamma$ radiation was carried out with $^{60}$Co at room temperature. The irradiation dose was 200 kGy at a dose rate of 48.6 kGy/h. After irradiation, the quantitative polymer formation was checked by IR spectroscopy and used for the X-ray structure analysis.

Poly((*Z*,*Z*)-**4**): colorless plates, insoluble in all solvents, mp 293 °C; IR (KBr) 1719 ($\nu_{C=O}$), 982 ($\nu_{C=C}$) cm$^{-1}$; powder X-ray 2$\theta$ (deg) 4.98, 10.38, 15.07, 16.11, 18.74, 21.71, 22.45, 25.08, 26.30, 27.38, 31.71, 33.10, 37.97, and 38.80.

Poly((*Z*,*Z*)-**6**): colorless plates, insoluble in all solvents, mp 300 °C; IR (KBr) 1719 ($\nu_{C=O}$), 982 ($\nu_{C=C}$) cm$^{-1}$; powder X-ray 2$\theta$ (deg) 4.80, 10.25, 14.60, 15.67, 18.33, 21.24, 21.99, 24.60, 25.98, 26.87, 30.77, 32.34, 37.91, and 38.61.

**Kinetic Analysis.** A change in the concentrations of the monomer and the polymer allowed us to assume Lambert−Beer's law,

$$A_1 = \epsilon_1 b C_1 \quad (2)$$

$$A_2 = \epsilon_2 b C_2 \quad (3)$$

where $A$ is the absorbance, $\epsilon$ is the absorption coefficient, $b$ is the path length, and $C$ is the fraction of the components. Subscripts 1 and 2 mean those for the monomer and polymers, respectively. Because summation of $C_1$ and $C_2$ is equal to unity, the following equation is obtained from eqs 2 and 3.

$$A_2 = -(\epsilon_2/\epsilon_1)A_1 + \epsilon_2 b \quad (4)$$

From eqs 2−4, the $C_1$ can be evaluated as follows:

$$C_1 = 1/\{(A_2/A_1)(\epsilon_1/\epsilon_2) + 1\} \quad (5)$$

The $A_2$ values derived from the 982 and 718 cm$^{-1}$ bands are plotted versus the $A_1$ values from the 1593 cm$^{-1}$ band. The values of $\epsilon_1/\epsilon_2$ are obtained from the slope of the straight lines. The $C_1$ values are calculated from eq 6, and the results are shown in Figure 4 as a function of the UV irradiation time. The logarithm of $C_1$ linearly decreased versus the irradiation time.

$$-(dC_1/dt) = kC_1 \quad (6)$$

$k$ is the rate constant, and $t$ is the UV irradiation time.

**X-ray Crystallography.** Single-crystal X-ray data for (*Z*,*Z*)-**4** and (*Z*,*Z*)-**6**-I at room temperature were collected on a Nonius Kappa CCD system using Mo K$\alpha$ radiation monochromated by graphite. Data for (*Z*,*Z*)-**1** and (*E*,*E*)-**1** were collected on a DIP3000 imaging plate diffractometer, Mac Science Co. Ltd., Japan. The structures were solved by a direct method with the program SIR92 and refined by full-matrix least-squares procedures. All calculations were performed using maXus from Mac Science. The analysis for (*Z*,*Z*)-**6**-I was carried out with an isotropic temperature factor, since it was difficult to complete the structure analysis. Single-crystal X-ray data for the (*Z*,*Z*)-**4** at −120 °C and other crystals were collected on a Rigaku AFC7R four-circle diffractometer or a Rigaku R-AXIS RAPID Imaging Plate diffractometer using Mo K$\alpha$ radiation ($\lambda$ = 0.71073 Å) monochromated by graphite. The structures were solved by a direct method with the programs SIR88 and SIR92 and refined using full-matrix least-squares procedures. All calculations were performed using the teXsan and CrystalStructure crystallographic software package of the Molecular Structure Corporation. Some hydrogen atoms were refined by differential Fourier calculation, and their positions were isotropically refined. The remaining hydrogen atoms were located on the calculated position with a distance of 0.95 Å.

**Acknowledgment.** This work was supported by PRESTO-JST (Conversion and Control by Advanced Chemistry) and also by Grant-in-Aids for Scientific Research (nos. 11650911 and 13450381) from the Ministry of Education, Culture, Sports, Science, and Technology of Japan. The authors acknowledge Dr. Kunio Oka, Research Institute for Advanced Science and Technology, Osaka Prefecture University, for permission to use the $\gamma$-radiation facilities.

**Supporting Information Available:** X-ray crystallographic data for all muconic esters (CIF). This material is available free of charge via the Internet at http//pub.acs.org.

JA0205333